Structure of the Tertiary Complex of the RepA Hexameric Helicase of Plasmid RSF1010 with the ssDNA and Nucleotide Cofactors in Solution †

ARTICLE *in* BIOCHEMISTRY · DECEMBER 2007

Impact Factor: 3.02 · DOI: 10.1021/bi700729k · Source: PubMed

Structure of the Tertiary Complex of the RepA Hexameric Helicase of Plasmid RSF1010 with the ssDNA and Nucleotide Cofactors in Solution†

Agnieszka Marcinowicz, Maria J. Jezewska, Paul J. Bujalowski, and Wlodzimierz Bujalowski*

Department of Biochemistry and Molecular Biology, Department of Obstetrics and Gynecology, The Sealy Center for Structural Biology, and The Sealy Center for Cancer Cell Biology, The University of Texas Medical Branch at Galveston, 301 University Boulevard, Galveston, Texas 77555-1053

Received April 17, 2007; Revised Manuscript Received June 19, 2007

ABSTRACT: The structure of the complex of the hexameric replicative helicase RepA protein of plasmid RSF1010 with ssDNA has been examined using the fluorescence energy transfer and analytical ultracentrifugation methods. We utilized the fact that the RepA monomer contains a single, natural cysteine residue. The cysteine residue has been modified with a fluorescent marker, which serves as the donor to the acceptor placed in different locations on the DNA. Using the two independent fluorescence donor−acceptor pairs and different DNA oligomers, we provide direct evidence that, in the complex with the enzyme, the ssDNA passes through the inner channel of the RepA hexamer. In the stationary complex, the RepA hexamer assumes a strictly single orientation with respect to the polarity of the sugar−phosphate backbone of the nucleic acid, with the large domain of protomers facing the 3′ end of the bound DNA. Interactions with the helicase induce profound changes in the structure of the bound DNA, and these changes are predominantly localized in the proper DNA-binding site. The heterogeneity of the structure of the bound DNA reflects the heterogeneous structure of the total RepA helicase DNA-binding site. This is in excellent agreement with the thermodynamic data. The structure of the RepA hexamer, in solution, differs considerably from the crystal structure of the enzyme. Both fluorescence energy transfer and analytical ultracentrifugation data indicate a significant conformational flexibility of the RepA hexamer. Implications of these results for the mechanism of interactions of the hexameric helicase with the DNA are discussed.

Fundamental processes of DNA and RNA metabolism, like replication, recombination, repair, and translation, require that the duplex structure of the nucleic acid be unwound to form a transiently metabolically active single-strand DNA intermediate (*1*−*5*). This reaction is fueled by the hydrolysis of nucleoside triphosphates and catalyzed by a class of enzymes called helicases (*3*−*5*). The RepA protein is one of several proteins encoded by broad host nonconjugative plasmid RSF1010, which can replicate in most Gram-negative bacteria and confers bacterial resistance to sulfonamides, and streptomycin (*6*−*11*). The RepA enzyme is the DNA replicative helicase, which is essential for RFS1010 plasmid replication in bacterial cells unwinding the dsDNA in a 5′ → 3′ direction (*8*−*11*). The molecular mass of the RepA monomer is 29 896 Da; i.e., it is one of the smallest known helicases. In the crystal, the RepA helicase forms a dimer of two ringlike hexameric structures, i.e., a dodecamer, although, under neutral and slightly alkaline conditions, in solution, the protein exclusively exists as a very stable hexamer (*11*). The RepA hexamer has a ringlike structure with a central cross channel ∼17 Å in diameter, as depicted in Figure 1. Both the hexamer and the dodecamer have helicase activity (*8*). In terms of stability, the RepA hexamer resembles the *Escherichia coli* primary replicative helicase, the DnaB protein, which requires only magnesium cations to preserve the integrity of the hexamer (*12*−*19*). Similar ringlike structures have been found for other well-studied replicative hexameric helicases, like bacteriophage T4 and T7 and the *E. coli* transcription termination factor Rho helicase, although these enzymes require a nucleotide cofactor and/or DNA to stabilize the hexameric structure (*20*−*22*).

Functional homology, high stability, and nucleic acid binding properties of the RepA hexamer resemble the behavior of the hexamer of the *E. coli* DnaB helicase (*12*, *14*, *15*, *17*). The total site size of the RepA hexamer−ssDNA[1] complex is 19 ± 1 nucleotide residues, as compared to 20 ± 3 for the DnaB hexamer−ssDNA complex (*23*). The total DNA-binding sites of both hexamers have heterogeneous structures (*12*, *14*, *15*, *17*, *23*). In the case of the RepA helicase, part of the total binding site constitutes the proper ssDNA-binding site of the enzyme, an area that possesses a strong ssDNA binding capability and encompasses up to ∼11 nucleotides of the ssDNA (*23*). The proper ssDNA-binding subsite is structurally separated from the remaining part of

† This work was supported by NIH Grant GM-46679 (to W.B.).

* To whom correspondence should be addressed. Telephone: (409) 772-5634. Fax: (409) 772-1790. E-mail: wbujalow@utmb.edu.

[1] Abbreviations: AMP-PNP, β,γ-imidoadenosine 5′-triphosphate; Tris, tris(hydroxymethyl)aminomethane; EM, electron microscopy; CP, 7-(diethylamino)-3-(4′-maleimidylphenyl)-4-methylcoumarin; FLM, fluorescein 5-maleimide; Hepes, *N*-(2-hydroxyethyl)piperazine-*N*′-2-ethanesulfonic acid; DEAE-cellulose, diethylaminoethylcellulose; FITC, fluorescein 5′-isothiocyanate; ssDNA, single-stranded DNA; TRITC, tetramethylrhodamine-6-isothiocyanate.

10.1021/bi700729k CCC: $37.00
Published on Web 10/16/2007

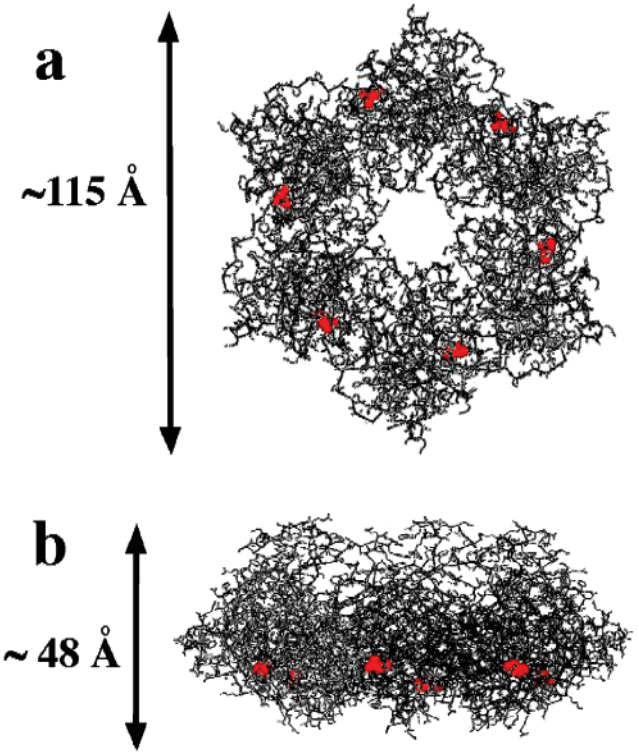

FIGURE 1: Structure of the RepA helicase hexamer determined in crystallographic studies (*10*). The structure has been generated using data from RCSB Protein Data Bank entry 1G8Y using ViewerPro (San Diego, CA). (a) The six subunits form a ringlike structure with a hexamer diameter of ~115 Å and with a central cross channel with a diameter of ~17 Å. (b) Side view of the RepA hexamer with the short perpendicular axis, of ~48 Å. Each protomer in the hexamer is built of two domains, large and small. The single cysteine residue in each protomer is located in the large domain and is colored red. All six cysteine residues lie in the plane perpendicular to the short axis of the RepA hexamer (see the text for details).

the total ssDNA-binding site. Surprisingly, while the engagement of the proper ssDNA-binding site in interactions with the ssDNA is accompanied by net ion release, the engagement of the total ssDNA-binding site of the RepA hexamer in interactions with the ssDNA results in an uptake of ions by the protein. Moreover, the proper ssDNA-binding site of the RepA enzyme shows a significant preference for pyrimidine oligomers, which is different from that of the *E. coli* DnaB hexamer which shows a significant preference for purine oligomers.

Formulating a mechanism of such a complex enzyme as the hexameric helicase requires knowledge of the structure of the helicase−ssDNA complex. For some hexameric helicases, including *E. coli* RuvB protein, archaeal MCM complex, or bacteriophage T7 helicase, the data indicated that, in the complex with the enzyme, the ssDNA passes through the cross channel of the protein hexamer (*24*−*26*). A similar mode of ss nucleic acid binding has been proposed for the hexamer of the SV40 T large antigen helicase and *E. coli* termination factor Rho helicase, although the mode of the nucleic acid binding has not been directly addressed and the modes of the ssDNA binding outside the cross channel have also been considered (*29*−*32*). In the case of the DnaB helicase, fluorescence energy transfer analyses directly indicated the ssDNA passes through the cross channel of the hexamer (*18*). However, the cross channel of the DnaB helicase is ~40 Å in diameter and can easily accommodate even the dsDNA helix (*33*−*35*). The integrity of the hexameric structure requires magnesium, and such a controlled stability can facilitate the binding of the ssDNA in the cross channel, which occurs through the local opening of the dynamic hexameric structure (*12*, *36*). On the other hand, in the crystal structure, the diameter of the cross channel of the RepA hexamer is dramatically smaller and the hexameric structure of the enzyme exhibits exceptional stability, not affected by solution conditions and/or nucleotide and DNA binding. This behavior is very different from that of other analogous and much larger hexameric helicases, which require Mg^{2+}, nucleotides, or a nucleic acid to stabilize the hexameric structure (*20*−*22*). The mechanism from the ssDNA to the RepA helicase is still unknown.

Functional and structural homology between the RepA hexamer and the *E. coli* primary replicative helicase, the DnaB protein, makes the RepA protein an excellent model for comparative studies. Moreover, the fact that the protein is essential for RSF1010 plasmid replication suggests some specific mechanism of RepA hexamer activity, which is not yet known. Furthermore, the essential role of the protein in replication of RSF1010, a ubiquitous multiple-copy plasmid, conferring resistance to antibiotics, provides an opportunity to examine molecular aspects of such resistance (*7*). Quantitative information about the complex of the RepA hexamer with the DNA is an absolute prerequisite for formulating any model of the enzyme activity and a hexameric helicase, in general.

In this paper, we present direct evidence that, in the complex with the RepA hexamer, the ssDNA passes through the cross channel of the enzyme. The heterogeneity of the total DNA-binding site of the enzyme is reflected in the profound heterogeneous changes in the structure of the bound DNA, particularly localized in the proper DNA-binding site. The RepA hexamer binds the ssDNA in a strictly single orientation with respect to the polarity of the sugar−phosphate backbone of the nucleic acid. In the complex, the hexamer is strictly oriented with its large domain toward the 3′ end of the bound DNA. The RepA hexamer has a dynamic structure, and its global structure, in solution, profoundly differs from the structure determined in crystallographic studies.

MATERIALS AND METHODS

Reagents and Buffers. All chemicals were reagent grade. All solutions were made with distilled and deionized >18 MΩ (Milli-Q Plus) water. Spectroscopic and binding experiments were performed in buffer T5 which is 50 mM Tris adjusted to pH 7.6 with HCl at 10 °C, 1 mM $MgCl_2$, 10 mM NaCl, 0.5 mM AMP-PNP, and 10% glycerol (*23*).

RepA Helicase of Plasmid RSF1010. The gene of the RepA helicase has been isolated directly from plasmid RSF1010 and placed in plasmid pET30a under control of the T7 polymerase system. Isolation and purification of the protein were performed, with slight modifications, as described previously (*8*, *23*). The protein was >99% pure as judged by SDS−acrylamide gel electrophoresis with Coomassie Brilliant Blue staining. The concentration of the protein was spectrophotometrically determined using an extinction coefficient ϵ_{280} of 1.656×10^5 cm^{-1} M^{-1}, obtained with the approach based on Edelhoch's method (*37*, *38*).

Nucleic Acids. All nucleic acids were purchased from Midland Certified Reagents (Midland, TX). The ssDNA 10-mer, $dT(pT)_9$, and 20-mer, $dT(pT)_{19}$, labeled with fluorescein at the 5′ end, or at a different location of the nucleic acid, were synthesized using fluorescein phosphoramidate. Labeling of 10- and 20-mers at the 3′ end with fluorescein, or labeling with rhodamine (Rho), was performed by synthesizing $dT(pT)_{19}$ with a nucleotide residue in a given location of the nucleic acid with the amino group on a six-carbon linker and, subsequently, modifying the amino group with FITC or TRITC (Midland Certified Reagents). The degree of labeling was determined by the absorbance at 494 nm for fluorescein (pH 9) using an extinction coefficient ϵ_{494} of 7.6×10^4 M^{-1} cm^{-1} and at 555 nm for rhodamine using an extinction coefficient ϵ_{555} of 8.0×10^4 M^{-1} cm^{-1} (*17*, *18*). Concentrations of all ssDNA oligomers have been spectrophotometrically determined, as previously described by us (*12*−*19*).

Labeling the RepA Hexamer with Coumarin (CP). Labeling of the cysteine residues of the RepA hexamer with CP was performed in H buffer [50 mM Hepes-HCl (pH 8.1), 100 mM NaCl, 5 mM $MgCl_2$, and 10% glycerol] at 4 °C (*17*, *18*). The fluorescent label was added from the stock solution to a dye/RepA molar ratio of ≈25. The mixture was incubated for 4 h, with gentle mixing. After incubation, the protein was precipitated with ammonium sulfate and dialyzed overnight against buffer T5. Any remaining free dye was removed from the modified RepA-CP by applying the sample to a DEAE-cellulose column and eluting with buffer T5 containing 500 mM NaCl. The degree of labeling, γ, was determined by the absorbance of a marker using an extinction coefficient ϵ_{394} of 27×10^3 M^{-1} cm^{-1} (*17*, *18*). The obtained values of γ were 0.31 ± 0.05 per hexamer, indicating that only a fraction of the cysteine residues in RepA hexamer are readily available for modification (see below). The labeled RepA protein is termed RepA-CP.

Analytical Ultracentrifugation Measurements. Analytical ultracentrifugation experiments were performed with an Optima XL-A analytical ultracentrifuge (Beckman Inc., Palo Alto, CA) using double-sector charcoal-filled 12 mm centerpieces as we previously described (*12*, *15*, *23*, *39*−*42*). Sedimentation velocity scans were collected at the absorption band of the RepA helicase at 280 nm. The RepA helicase−nucleotide complexes were scanned at 295 nm where the cofactor absorbance is minimal and the absorbance of the sample is dominated by the protein (*12*). Moreover, the reference compartment contained the same concentration of the cofactor as the protein−nucleotide complex. Time derivative analyses of sedimentation scans were performed with the software supplied by the manufacturer using an average of eight to fifteen scans for each concentration as previously described (*43*, *44*). The values of sedimentation coefficients were corrected to $s_{20,w}$ for solvent viscosity and temperature to standard conditions (*45*, *46*).

Fluorescence Measurements. All steady-state fluorescence measurements were performed using the Fluorolog-3 spectrofluorometer (Jobin Yvon, Edison, NJ) as previously described (*12*−*19*, *47*−*51*). To avoid possible artifacts, due to the fluorescence anisotropy of the sample, polarizers were placed in excitation and emission channels and set at 90° and 55° (magic angle), respectively (*52*, *53*). Computer fits were performed using Mathematica (Wolfram) and KaleidaGraph (Synergy Software, Reading, PA).

Determination of the Average Efficiency of Fluorescence Energy Transfer from the Donor on the RepA Hexamer to the Acceptor Located on the DNA. The efficiency of the fluorescence radiationless energy transfer, *E*, from the donor, located on the RepA protein, to an acceptor, located on the DNA bound in the DNA-binding site of the helicase, has been determined using two independent methods. The fluorescence of the donor in the presence of the acceptor, F_{DA}, is related to the fluorescence of the same donor, in the absence of the acceptor, F_D, by (*13*, *15*, *17*, *18*, *54*)

$$F_{DA} = (1 - \nu_D)F_D + F_D\nu_D(1 - E_D) \quad (1)$$

where ν_D is the fraction of donors in the complex with the acceptor and E_D is the average efficiency of fluorescence energy transfer from a donor to an acceptor, determined from the quenching of the donor fluorescence emission. Thus, the average transfer efficiency, E_D, obtained from the quenching of the donor fluorescence emission is obtained by rearranging eq 1 as

$$E_D = \left(\frac{1}{\nu_D}\right)\left(\frac{F_D - F_{DA}}{F_D}\right) \quad (2)$$

The value of ν_D has been determined using the binding constant for a given DNA oligomer for the RepA helicase, measured under the same solution conditions (see below) (*23*).

In the second independent method, the average fluorescence transfer efficiency, E_A, has been determined using the sensitized acceptor fluorescence emission, by measuring the fluorescence intensity of the acceptor (fluorescein or rhodamine), excited at a wavelength where a donor (CP) predominantly absorbs, in the absence and presence of the donor (*52*). The fluorescence intensities of the acceptor in the absence, F_A, and presence of the donor, F_{AD}, are defined as (*13*, *15*, *17*, *18*, *54*)

$$F_A = I_o\epsilon_A C_{AT}\phi_F^A \quad (3)$$

and

$$F_{AD} = (1 - \nu_A)F_A + I_o\epsilon_A\nu_A C_{AT}\phi_B^A + I_o\epsilon_D C_{DT}\nu_D\phi_B^A E_A \quad (4)$$

where I_o is the intensity of incident light, C_{AT} and C_{DT} are the total concentrations of the acceptor and donor, respectively, ν_A is the fraction of acceptors in the complex with donors, ϵ_A and ϵ_D are the molar absorption coefficients of the acceptor and donor at the excitation wavelength, respectively, ϕ_F^A and ϕ_B^A are the quantum yields of the free and bound acceptor, respectively, and E_A is the average transfer efficiency determined by the acceptor-sensitized emission. All quantities in eqs 3 and 4 can be experimentally determined (*13*, *15*, *17*, *18*, *54*). Dividing eq 3 by eq 4 and rearranging provide the average transfer efficiency, E_A, as

$$E_A = \left(\frac{1}{\nu_D}\right)\left(\frac{\epsilon_A C_{AT}}{\epsilon_D C_{DT}}\right)\left[\left(\frac{\phi_F^A}{\phi_B^A}\right)\left(\frac{F_{AD}}{F_A}\right) + \nu_A + \nu_A\left(\frac{\phi_F^A}{\phi_B^A}\right) - 1\right] \quad (5)$$

It should be pointed out that the energy transfer efficiencies, E_D and E_A, are apparent quantities. E_D is a fraction of the photons absent in the donor emission as a result of the presence of an acceptor, including transfer to the acceptor and possible nondipolar quenching processes, induced by the presence of the acceptor, and E_A is a fraction of all photons absorbed by the donor, which were transferred to the acceptor. The true Förster energy transfer efficiency, E, is a fraction of the photons absorbed by the donor and transferred to the acceptor, in the absence of any additional nondipolar quenching resulting from the presence of the acceptor (*42*, *52*, *55*). The value of E is related to the apparent quantities of E_D and E_A by (*42*, *55*)

$$E = \frac{E_A}{1 - E_D + E_A} \tag{6}$$

Thus, measurements of the transfer efficiency, using both methods, are not alternatives but parts of the complete analysis that yields the true efficiency of the fluorescence energy transfer process (*42*, *52*, *54*). The efficiency of fluorescence energy transfer between the donor and acceptor dipoles is related to the distance, R, separating the dipoles by the relationships (*52*)

$$E = \frac{R_o^6}{R_o^6 + R^6} \tag{7}$$

and

$$R = R_o\left(\frac{1 - E}{E}\right)^{1/6} \tag{8}$$

where $R_o = 9790(\kappa^2 n^{-4} \phi_d J)^{1/6}$ and is the so-called Förster critical distance (in angstroms), the distance at which the transfer efficiency is 50%, κ^2 is the orientation factor, ϕ_d is the donor quantum yield in the absence of the acceptor, and n is the refractive index of the medium ($n = 1.4$). The overlap integral, J, characterizes the resonance between the donor and acceptor dipoles and has been evaluated by integration of the mutual area of overlap between the donor emission spectrum, $F(\lambda)$, and the acceptor absorption spectrum, $\epsilon(\lambda)$ (*52*). The values of R_o have been determined, as previously described by us, and are 52 and 47 Å for the coumarin−fluorescein and coumarin−rhodamine systems, respectively (*15*, *17*, *18*).

The fluorescence transfer efficiency determined for a single donor−acceptor pair depends on the distance between the donor and the acceptor, R, and the factor κ^2, describing the mutual orientation of the donor and acceptor dipoles (*52*). The factor κ^2 cannot be experimentally determined but can assume a value from 0 to 4. For a complete random orientation of the acceptor and donor, $\kappa^2 = 0.67$. However, because the distance between a donor and an acceptor depends upon the one-sixth power of κ^2, only the two extreme values (0 or 4) would significantly affect the determined distance. The available analysis of the possible range of distances between the donor and the acceptor describes the situation in which only a single donor−acceptor pair is used (*56*). However, as we discussed before, another equally rigorous procedure for empirically evaluating the error in the distance determination, although more time-consuming and much more expensive, is to use more than one different donor−acceptor pair and/or donor and acceptor placed in different locations (*18*, *54*). The different molecular structures of different donors and acceptors and/or different locations introduce an intrinsic randomization of the orientation of the absorption and emission dipoles. The measurement of a similar distance, using different donor−acceptor pairs, indicates that the orientation of the donor and absorption dipoles is far from the extreme values of 0 or 4 and that the true distance between a donor and an acceptor is represented by the distance obtained using a κ^2 of 0.67 (see below) (*18*, *54*).

RESULTS

Labeling of the Cysteine Residues of the RepA Hexamer. As mentioned above, the RepA monomer contains a single cysteine residue (C172) (*10*). The crystal structure of the RepA hexamer, with locations of the native cysteine residues in the three-dimensional structure of the protein, is depicted in panels a and b of Figure 1. The largest diameter and side length of the RepA hexamer observed in its crystal structure are ∼115 and ∼48 Å, respectively. The structure of each protomer has an elongated shaped and is built of two domains, small and large. The cysteine residues are located close to one end of the hexamer within the large domain (Figure 1b). The asymmetric location of the cysteine residues facilitates the interpretations of the fluorescence energy transfer data (see below). Nevertheless, although the crystal structure suggests that all cysteine residues are equally exposed to the solvent, the maximum achievable degree of labeling, γ, with coumarin maleimide (CP), which is very specific for the thiol groups, is 0.31 ± 0.05 CP molecule per hexamer. This value could not be increased by the increased concentration of the marker or by the prolonged time of incubation, limited by the protein precipitation or the loss of enzyme activity. Thus, only one cysteine residue, in the solution structure of the RepA hexamer, is partially accessible for labeling, or all six cysteine residues are labeled, but to a lesser degree. This is very different from the analogous labeling of native cysteine residues of the *E. coli* transcription termination factor Rho hexamer, where all six cysteine residues are accessible to the marker (*57*). The limited degree of labeling does not affect the fluorescence energy transfer experiments or their analyses, which we describe in the context of labeling a single cysteine residue. Nevertheless, it indicates that the structure of the RepA hexamer, in solution, is different from its crystal structure (see the Discussion). Direct evidence that this is the case comes from the fluorescence energy transfer and analytical ultracentrifugation studies described below.

Theoretical Analysis of the Efficiency of Fluorescence Energy Transfer between the Donor, Located on the Ring of Six Identical Sites of the Protein Hexamer, and the Acceptor, Placed at Any Location on the Bound DNA. The RepA hexamer binds a single ssDNA 20-mer molecule, which occupies the total DNA-binding site of the enzyme (*23*). There are two fundamentally different structural models, which can describe the complex between the RepA hexamer and the bound ssDNA 20-mer (*18*, *24*−*32*). These two models are schematically depicted in panels a and b of Figure 2. In the first model, in Figure 2a, the nucleic acid passes through the cross channel of the protein hexamer. In this

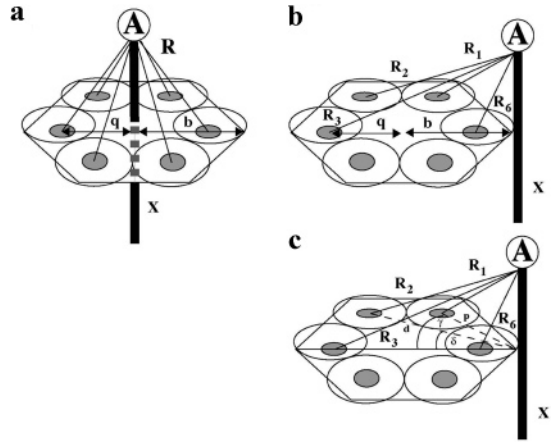

FIGURE 2: (a) Schematic diagram showing the arrangement of a plane with a ring of six cysteine residues, each being a possible location site of a single fluorescence energy transfer donor and a single acceptor located along a nucleic acid lattice, bound in the inner channel of the hexamer (*18*). The acceptor can be located above and below the plane with the donor. The distance from the acceptor to the plane of the ring of donors is designated as *x*. The distance, *R*, from the acceptor to each donor is the same for all six donors (see the text for details). (b) Schematic diagram showing the arrangement of a plane with a ring of six cysteine residues, each being a possible location site of a single fluorescence energy transfer donor and a single acceptor located along the ss nucleic acid bound to the outside of one the protomers of the hexamer. The acceptor can be placed above or below the plane with the donor. The distance from the acceptor to the plane of the ring of donors is designated as *x*. The possible different distances from the particular location of the donor to the acceptor are R_1, R_2, R_3, and R_6 (see the text for details). (c) Geometrical relationships among the distance from the particular donor location to the center of the hexamer, *q*, the radius of the hexamer, *b*, and the particular distances between the donor and the acceptor located along the nucleic acid lattice bound on the outside to one of the protomers of the hexamer, *p*, *d*, R_1, R_2, R_3, and R_6 (see the text for details).

model, every possible location of the donor on the RepA hexamer is an approximately similar distance from each base of the bound ssDNA oligomer. In the second model, in Figure 2b, the nucleic acid binds to the single DNA-binding site on one of the protomers, on the outside surface of the hexamer. Unlike the first model, there are large differences among the distances between a given base in the nucleic acid and the possible locations of the donor on the hexamer (see below).

There are several constraints we can use in our analysis. First, the ringlike structure of the crystal structure of the RepA hexamer has a diameter of ∼115 Å, with the inner channel of the hexamer having a diameter of ∼17 Å (Figure 1a,b) (*10*). The distance between the opposing cysteine residues in the hexamer is ∼70 Å. Moreover, the cysteine residues are in the plane perpendicular to the axis of the hexamer (Figure 1b). These dimensions indicate that the distance from the center of the hexamer to the outside surface of the protomers in the hexamer is in the range of ∼60−80 Å. Second, the Förster critical distances, R_o, for the used donor−acceptor pairs are around 50 Å (Materials and Methods) (*15*, *17*, *18*). Third, independent measurements of the structure of the ssDNA 20-mer, labeled at its 5′ and 3′ ends with a fluorescence donor and an acceptor, in the complex with the RepA hexamer, indicate that the length of the bound oligomer is ∼75 Å (data not shown). Because the fluorescence markers contribute to the length of the oligomer as two additional bases, this distance is very close to the length of one strand of dsDNA, 22 bp long, in the B form (∼78 Å) (*18*, *58*, *59*). Thus, in our fluorescence energy transfer analyses, the size of the RepA hexamer, R_o, of the used donor−acceptor pairs and the length of the nucleic acid impose a set of constraints on the possible distances between the donors and acceptors and the values of the average energy transfer efficiencies (see below).

First, we address the situation in which a single acceptor is located in any position along a nucleic acid lattice bound in the cross channel of the hexamer (Figure 2a). In other words, the acceptor can be placed above and below the plane, in which the donor is located on the hexamer. Such a situation corresponds to the fluorescence energy transfer process in the complexes of RepA-CP with $dT(pT)_{19}$ labeled with fluorescein or rhodamine at different locations along the nucleic acid, described below. The distance between the acceptor placed in an arbitrary location on the ss nucleic acid, with respect to the plane of the donor, is designated as *x*. For the DNA bound in the cross channel of the hexamer (Figure 2a), the single donor can be located at any specific site on each protomer. In each possible site, the donor is the same distance from the center of the hexamer, *q*, and the same distance, *R*, from the acceptor on the nucleic acid. The acceptor can be located any distance, *x*, from the plane of donor. The values of *R* and *x* are described by the Pythagorean theorem

$$R = (x^2 + q^2)^{0.5} \tag{9}$$

The average value of *E* as a function of *R* is then described by eq 7.

The theoretical dependence of the average fluorescence energy transfer efficiency, *E*, as a function of the average distance from the acceptor to the plane with the donor, *x*, and for different distances from the donor to the center of the hexamer, *q*, is shown in Figure 3a. The selected value of R_o is 52 Å and corresponds to the CP (donor)−fluorescein (acceptor) system (*17*, *18*). In these calculations, we allowed the nucleic acid to protrude from both sides of the plane with the donor, within the full length of the ssDNA 20-mer, i.e., ∼70 Å. This is a useful although not absolutely necessary generalization, because the thermodynamic studies clearly showed that the ssDNA 20-mer assumes a well-defined location within the total DNA-binding site of the helicase (*23*). For different values of *q*, as the acceptor moves along the nucleic acid, the plots span different regions of the average distance, *R* (Figure 2a), and correspondingly different values of the average fluorescence energy transfer efficiency, *E*. When $q = 60$ Å, the donor would be as far as the diameter of the crystal structure of the RepA hexamer (Figure 1a), and the maximum value of the energy transfer efficiency can be only ∼0.29 and corresponds to the acceptor located in the plane with the donor. For different values of *q*, as the donor approaches the center of the hexamer, the possible maximum value of *E* increases. For *q* values in the range of 35−50 Å, which corresponds to the distance from the cysteine residues to the center of the hexamer in the crystal structure of the RepA protein (Figure 1a,b), the maximum values of the average fluorescence energy transfer efficiency reach values in the range of ∼0.5−0.9. Another characteristic feature of the plots in Figure 3a, obtained for *q* values

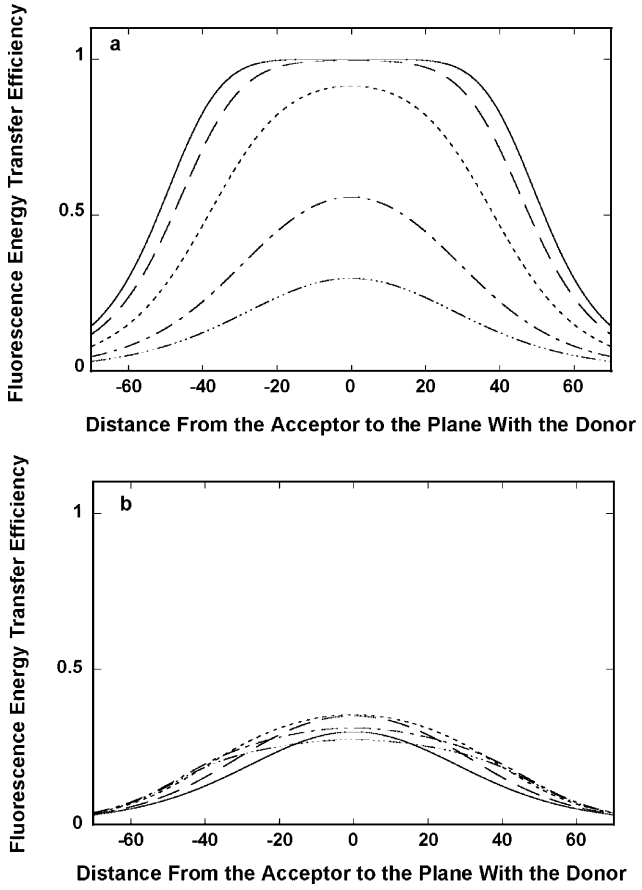

FIGURE 3: (a) Theoretical dependence of the average efficiency, E, of Förster fluorescence energy transfer from a single donor, placed at any of the six possible cysteine residues of the RepA hexamer, to a single acceptor located along the ss nucleic acid bound in the cross channel of the hexamer on the average distance from the acceptor to the plane with the donor, x (Figure 2a). The plots were generated using eqs 7 and 9 for different distances between the donor and the center of the hexamer, q. The maximum distance from the outside surface of the hexamer to its center, i.e., the selected radius of the hexamer (b), equals 60 Å, and the maximum selected length of the nucleic acid (x) equals 70 Å. The critical Förster distance for the donor−acceptor pair is 52 Å: $q = 60$ Å (−•••−), $q = 50$ Å (− - −), $q = 35$ Å (- - -), $q = 20$ Å (− − −), and $q = 1$ Å (—). (b) Theoretical dependence of the average efficiency, E, of Förster fluorescence energy transfer from a single donor, placed at any of the six possible cysteine residues of the RepA hexamer, to a single acceptor located along the ss nucleic acid bound on the outside of the hexamer on the average distance from the acceptor to the plane with the donor, x (Figure 2a). The plots were generated using eqs 7, 10, and 12 for different distances between the donor and the center of the hexamer, q. The maximum distance from the outside surface of the hexamer to its center, i.e., the selected radius of the hexamer (b), equals 60 Å, and the maximum selected length of the nucleic acid (x) equals 70 Å. The critical Förster distance for the donor-accepted pair is 52 Å: $q = 60$ Å (−•••−), $q = 50$ Å (− - −), $q = 35$ Å (- - -), $q = 20$ Å (− − −), and $q = 1$ Å (—).

between 35 and 50 Å, is the sharp decrease in the fluorescence energy transfer efficiency once the distance from the acceptor to the plane with the donor exceeds ~20 Å.

The behavior of the model where the nucleic acid binds on the outside of the hexamer, to one of the protomers, as depicted in Figure 2b, is very different. The donor can be located at any specific location on each protomer of the RepA hexamer and the same distance, q, from the center of the hexamer. The ssDNA is now tangent to the outside surface of one of the protomers. The geometry of this model is more complex than the geometry of the one previously considered and is shown in Figure 2c. Inspection of panels b and c of Figure 2 shows that the distance between the acceptor on the nucleic acid and the donor varies significantly for each particular location of the donor. For the set of m possible locations of a single fluorescence energy transfer donor, which is transferring energy to a single acceptor, the average value of E is weighted by the contributions from all possible locations of the donor and is defined, in general, as (*60*)

$$E = \left(\frac{1}{m}\right)\sum E_i \tag{10}$$

where E_i is the transfer efficiency from a particular location, i, of the donor to the acceptor and is defined by eq 7, for a particular distance, R_i. The average distance between the acceptor and the donor is analogously defined as

$$R_{\mathrm{av}} = \left(\frac{1}{m}\right)\sum R_i \tag{11}$$

In our case, $m = 6$. However, R_1, R_2, R_3, R_4, R_5, and R_6, the particular distances between a given location of the donor and the acceptor placed on the ssDNA, are now defined as (Figure 2c)

$$R_1 = (x^2 + p^2)^{0.5} \tag{12a}$$

$$R_2 = (x^2 + d^2)^{0.5} \tag{12b}$$

$$R_3 = [x^2 + (q + b)^2]^{0.5} \tag{12c}$$

$$R_4 = R_2 \tag{12d}$$

$$R_5 = R_1 \tag{12e}$$

$$R_6 = [x^2 + (b + q)^2]^{0.5} \tag{12f}$$

where b is the radius of the hexamer, $p = (q/2)(3^{0.5}/\sin\gamma)$, $\gamma = 60 + \arctan\{[(q - b)/(q + b)] \times 3^{0.5}\}$, $d = (q/2)(3^{0.5}/\sin\delta)$, and $\delta = 30 + \arctan\{[(q - b)/(q + b)] \times 3^{-0.5}\}$. The geometrical relationships between the donor−acceptor distances, R_i, are shown in Figure 2c.

The theoretical dependence of the average fluorescence energy transfer efficiency, E, upon the average distance from the acceptor to the plane with the donor, x, for different distances from the donor to the center of the hexamer, q, is shown in Figure 3b, with a b of 60 Å and an R_o of 52 Å. Because of the complex relationship between the R_{av} and the particular donor−acceptor distance, R_i, the plots either are very close or superimpose on each other, contrary to the model in which the ssDNA passes through the inner channel of the hexamer (Figure 3a). In other words, in the considered model, different donor−acceptor configurations may result in the same average energy transfer efficiencies. However, the most important feature of the plots in Figure 3b is that, independent of the distance between the donor and the center of the hexamer and independent of where the acceptor is located on the nucleic acid, the average energy transfer efficiency never exceeds ~0.34. This dramatically lower value of E, as compared to the energy transfer efficiency obtained for the model in which ssDNA passes through the

inner channel of the hexamer, results from the fact that the average distance between the donor and acceptor is always significantly larger than R_o (52 Å) of the donor−acceptor pair. This is true for any value of *q*, any location of the acceptor on the DNA, or any placement of the nucleic acid in the DNA-binding site of the RepA hexamer (Figure 2b). Moreover, the plots in Figure 3b, obtained for *q* values between 35 and 50 Å, show only a gradual decrease of *E*, once the distance from the acceptor to the plane with the donor exceeds ~20 Å, a behavior very different from that of the model with the ssDNA passing through the cross channel of the hexamer (Figure 3a). Thus, it is evident that the two fundamentally different models of the RepA hexamer−ssDNA complex differ dramatically in the value of the average fluorescence energy transfer efficiency for an arbitrary distance from the donor to the center of the protein hexamer, *q*. Moreover, the size of these differences well exceeds the errors due to approximations applied in the analysis (see below and the Discussion).

Distances between Different Fluorescence Energy Transfer Acceptors Placed in Different Locations on the ssDNA Oligomers, Which Span the Total ssDNA-Binding Site of the RepA Helicase and the Donor Located on the RepA Hexamer. The fluorescence emission spectrum of CP strongly overlaps with the absorption spectra of fluorescein and rhodamine, which is reflected in large values for the Förster critical distance R_o, which indicate that the selected donor−acceptor pairs, CP−fluorescein and CP−rhodamine, provide the required resolution for the fluorescence energy transfer measurements of the RepA hexamer−ssDNA system (Materials and Methods). Thus, if the selected donor and acceptors are in the proximity of each other, efficient fluorescence energy transfer will occur (see below). To address the topology of the RepA hexamer−ssDNA complex, we first performed fluorescence energy transfer measurements of the distances between the donor, CP, located on one of the RepA protomers and the acceptor placed at different positions along the ssDNA oligomer. The ssDNA oligomers used in these studies are depicted in Figure 4a. The fluorescence energy transfer acceptor, A, fluorescein or rhodamine, has been placed at the 5′ and 3′ ends of the nucleic acid and at different locations separated by five nucleotides. Binding of all ssDNA oligomers to the RepA hexamer is characterized by a binding constant [$K = (3.1 \pm 0.4) \times 10^6$ M^{-1}] virtually the same as that for the binding of the unmodified form, dT(pT)$_{19}$ or dT(pT)$_{20}$ (data not shown) (*23*).

Fluorescence emission spectra of the complexes of RepA-CP with the ssDNA oligomer, dT(pT)$_3$-Flu-dT(pT)$_{14}$, the emission spectrum of the RepA-CP complex with dT(pT)$_{19}$, in the absence of the acceptor, and the emission spectrum of dT(pT)$_3$-Flu-dT(pT)$_{14}$, in the complex with the RepA helicase in the absence of the donor, are shown in Figure 5a. The total concentrations of the RepA helicase and RepA-CP are 3×10^{-7} M. The total concentrations of the labeled and unlabeled ssDNA oligomers are 1×10^{-6} M. The spectra have been recorded with the excitation at $\lambda_{ex} = 425$ nm, i.e., in the major absorption band of the donor, CP (*17*−*19*, *54*, *60*). The spectra in Figure 5a show that the presence of the acceptor (fluorescein) induces a significant quenching of the donor fluorescence. Correspondingly, there is an increase in the acceptor fluorescence emission in the presence

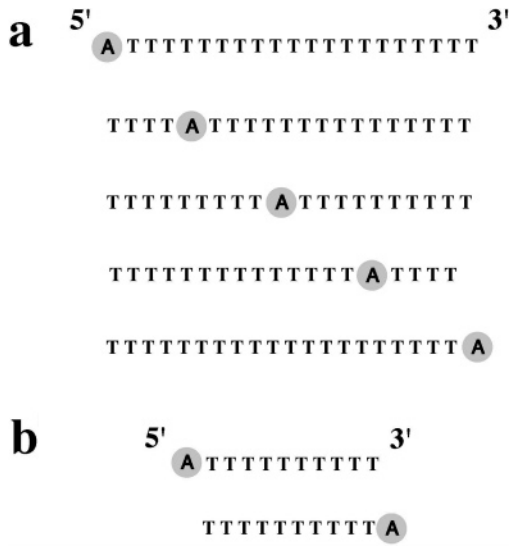

FIGURE 4: (a) Schematic primary structure of the ssDNA oligomers, dT(pT)$_{19}$, labeled with the fluorescence energy transfer acceptor. (a) fluorescein or rhodamine, at a different specific location on the ssDNA 20-mer used in fluorescence energy transfer experiments. In the case of fluorescein, the oligomers are designated in the text as 5′-Flu-dT(pT)$_{19}$ and dT(pT)$_3$-Flu-dT(pT)$_{14}$, and rhodamine oligomers are identified as 5′-Rho-dT(pT)$_{19}$, dT(pT)$_3$-Rho-dT(pT)$_{14}$, dT(pT)$_8$-Rho-dT(pT)$_9$, dT(pT)$_{13}$-Rho-dT(pT)$_4$, and dT(pT)$_{19}$-Rho-3′. These oligomers in the text are called 20-mers. (b) Schematic primary structures of the ssDNA oligomer, dT(pT)$_9$, labeled at the 5′ and 3′ ends with the fluorescence energy transfer acceptor, fluorescein or rhodamine. The labeled oligomers are designated in the text as 5′-Flu-dT(pT)$_9$, dT(pT)$_9$-Flu-3′, 5′-Rho-dT(pT)$_9$, and dT-(pT)$_9$-Rho-3′ and called 11-mers.

of the donor. Both features, the donor emission quenching and the sensitized acceptor emission, indicate that an efficient fluorescence energy transfer process occurs in the examined RepA−ssDNA oligomer system (*17*−*19*, *54*, *60*). Although the obtained data also indicate that formation of the complex between the protein and the nucleic acid affects the fluorescence intensity, it does not affect the shapes of the donor and the acceptor emission spectra.

The emission spectrum of the donor, in the complex with the acceptor, has been obtained by normalizing the peak of the spectrum of the donor, recorded in the absence of acceptor, to the intensity of the same donor recorded in the presence of the acceptor (Figure 5a). Subsequently, the emission spectrum of the acceptor in the complex with the donor has been obtained by subtracting the normalized emission spectrum of the donor from the emission spectrum of the complex containing both the donor and the acceptor. The normalized emission spectrum of the CP donor in the complex with the acceptor and the emission spectrum of the fluorescein acceptor in the complex with the donor, corresponding to the spectra in Figure 5a, are shown in Figure 5b, together with the emission of the donor and the acceptor, recorded in the absence of the corresponding fluorescence energy transfer partner. The emission intensities of the donor and acceptor alone and in the complex with the acceptor and the donor, respectively, have been obtained by integrating the emission spectra in Figure 5b. At the selected total concentrations of the enzyme and the nucleic acid, the degree of binding of the ssDNA oligomers to the RepA and RepA-CP (ν_D) and the degree of saturation of the nucleic acid with the helicase (ν_A) are ≈0.74 and ≈0.24, respectively, obtained using the binding constant [$K = (3.1 \pm 0.4) \times 10^6$ M^{-1}]

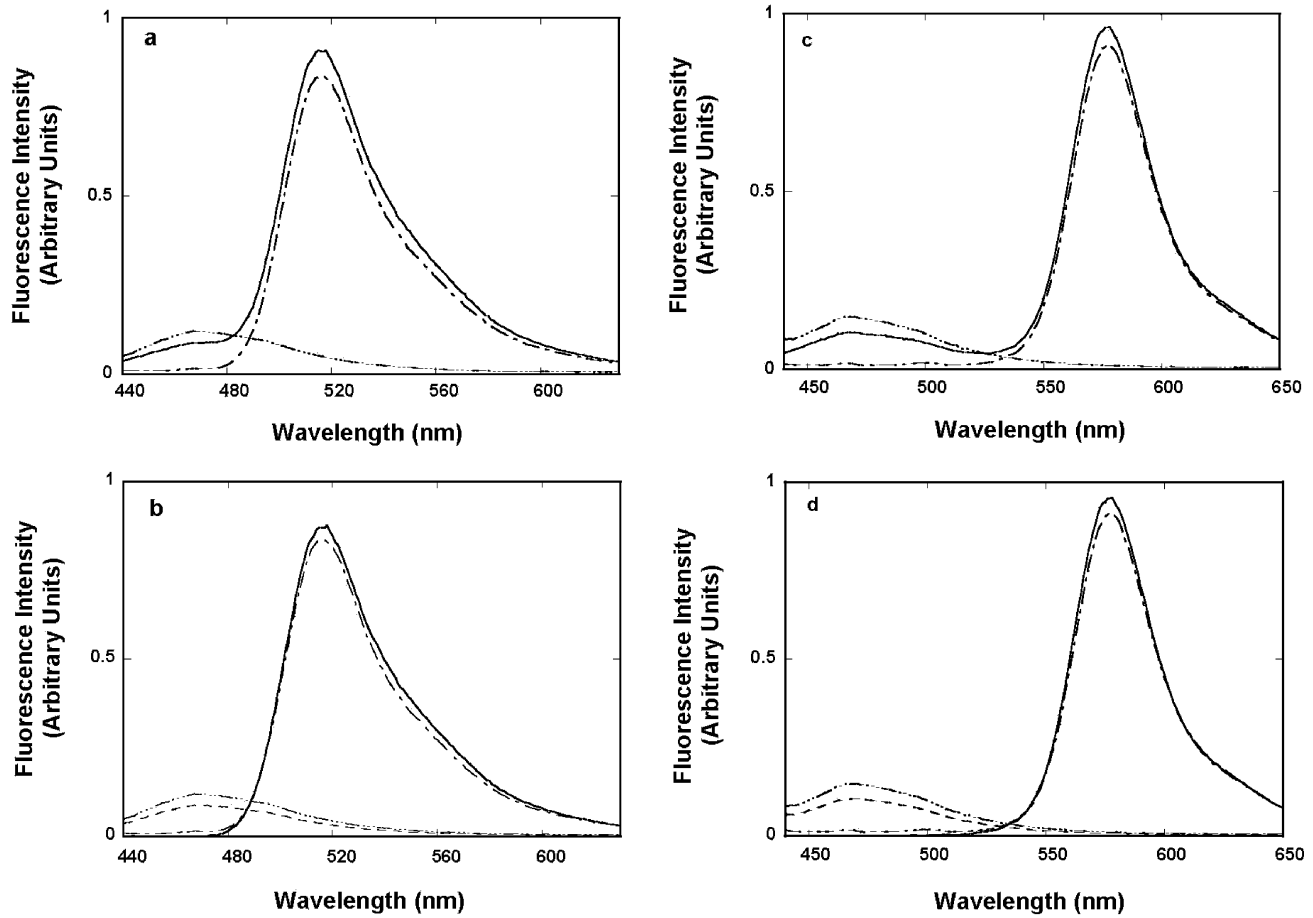

FIGURE 5: (a) Fluorescence emission spectrum ($\lambda_{ex} = 425$ nm) of the RepA hexamer, RepA-CP, labeled with the coumarin derivative, CP, in the presence of unlabeled $dT(pT)_{19}$ (−•••−), fluorescence emission spectrum of the ssDNA oligomer, $dT(pT)_3$-Flu-$dT(pT)_{14}$, in the presence of the unlabeled RepA hexamer (− - −), and fluorescence emission spectrum of the labeled RepA hexamer, RepA-CP, in the presence of the labeled ssDNA oligomer, $dT(pT)_3$-Flu-$dT(pT)_{14}$ (—), in buffer T5 (pH 7.6, 10 °C) containing 1 mM $MgCl_2$, 10 mM NaCl, 0.5 mM AMP-PNP, and 10% glycerol. Concentrations of RepA-CP and the ssDNA oligomer are 3×10^{-7} M (hexamer) and 1×10^{-6} M (oligomer), respectively (details in the text). (b) Fluorescence emission spectrum ($\lambda_{ex} = 425$ nm) of the labeled RepA hexamer, RepA-CP, in the presence of unlabeled $dT(pT)_{19}$ (−•••−), fluorescence emission spectrum of RepA-CP normalized to the emission of RepA-CP in a complex with $dT(pT)_3$-Flu-$dT(pT)_{14}$ (- - -), fluorescence emission spectrum of $dT(pT)_3$-Flu-$dT(pT)_{14}$ in the presence of the unlabeled RepA hexamer (− - −), and fluorescence emission spectrum of $dT(pT)_3$-Flu-$dT(pT)_{14}$ in a complex with RepA-CP, after subtraction of the normalized spectrum of RepA-CP in the same complex (—). Solution conditions and the concentrations of RepA-CP and the ssDNA oligomer are the same as those described for Figure 7a (details in the text). (c) Fluorescence emission spectrum ($\lambda_{ex} = 425$ nm) of the RepA hexamer, RepA-CP, labeled with coumarin, CP, in the presence of unlabeled $dT(pT)_{19}$ (−•••−), fluorescence emission spectrum of the ssDNA oligomer, $dT(pT)_3$-Rho-$dT(pT)_{14}$, in the presence of the unlabeled RepA hexamer (− - −), and fluorescence emission spectrum of the labeled RepA hexamer, RepA-CP, in the presence of the labeled ssDNA oligomer, $dT(pT)_3$-Rho-$dT(pT)_{14}$ (—), in buffer T5 (pH 7.6, 10 °C) containing 1 mM $MgCl_2$, 10 mM NaCl, 0.5 mM AMP-PNP, and 10% glycerol. Concentrations of RepA-CP and the ssDNA oligomer are 3×10^{-7} M (hexamer) and 1×10^{-6} M (oligomer), respectively (details in the text). (d) Fluorescence emission spectrum ($\lambda_{ex} = 425$ nm) of the labeled RepA hexamer, RepA-CP, in the presence of unlabeled $dT(pT)_{19}$ (−•••−), fluorescence emission spectrum of RepA-CP normalized to the emission of RepA-CP in a complex with $dT(pT)_3$-Rho-$dT(pT)_{14}$ (- - -), fluorescence emission spectrum of $dT(pT)_3$-Rho-$dT(pT)_{14}$ in the presence of the unlabeled RepA hexamer (− - −), and fluorescence emission spectrum of $dT(pT)_3$-Rho-$dT(pT)_{14}$ in the complex with RepA-CP, after subtraction of the normalized spectrum of RepA-CP in the same complex (—). Solution conditions and the concentrations of RepA-CP and the ssDNA oligomer are the same as those described for Figure 7c (details in the text).

characterizing the binding of the ssDNA 20-mers to the RepA helicase (*23*) (see above). The apparent fluorescence energy transfer efficiencies, E_D and E_A, the Förster fluorescence energy transfer efficiency, E, and the average distance between the donor and acceptor, $R(2/3)$, have then been calculated using eqs 2, 5, 6, and 8.

The same fluorescence energy transfer experiments have been performed for the entire series of ssDNA oligomers, depicted in Figure 4a, with fluorescein as the acceptor. The obtained fluorescence energy transfer efficiencies and corresponding average distances, $R(2/3)$, are included in Table 1. The value of E sharply increases from ~0.23 for 5′-Flu-$dT(pT)_{19}$ to ~0.42 and ~0.63 for $dT(pT)_3$-Flu-$dT(pT)_{14}$ and $dT(pT)_8$-Flu-$dT(pT)_9$, respectively. The corresponding average distance from the center of mass of the donor to the acceptor, $R(2/3)$, is ~63.4 Å for 5′-Flu-$dT(pT)_{19}$ and ~47.6 Å for $dT(pT)_8$-Flu-$dT(pT)_9$ (Table 1). However, a shift of the acceptor by an additional five nucleotides along the bound ssDNA in $dT(pT)_{13}$-Flu-$dT(pT)_4$ causes, not an increase, but a decrease in the value of E to ~0.54 and an increase of the average distance [$R(2/3)$] to ≈51 Å. A further shift of the acceptor to the 3′ end of the bound DNA in $dT(pT)_{19}$-Flu-3′ results in a dramatic decrease in the fluorescence energy transfer efficiency E to ~0.32 and a large increase in the average distance [$R(2/3)$] to ≈59 Å.

Recall that the measurement of the similar distance between the donor and the acceptor for different donor−acceptor pairs provides empirical evidence that the value of

Table 1: Fluorescence Energy Transfer Parameters of the Complexes of the Hexameric Helicase RepA of Plasmid RSF1010, Labeled with the Fluorescence Energy Transfer Donor, Coumarin, with Different ssDNA Oligomers, Containing a Fluorescence Energy Transfer Acceptor, Fluorescein, in Buffer T5 (pH 7.6, 10 °C)[a]

ssDNA oligomer	E_D	E_A	E	R_o (Å)	$R(2/3)$ (Å)	$R(2/3)_{av}$ (Å)[b]	x_{av}[b]
5′-Flu-dT(pT)$_{19}$	0.61 ± 0.04	0.12 ± 0.02	0.23 ± 0.03	52	63.4 ± 3.1	65.4 ± 3.1	44.3 ± 3.1
dT(pT)$_3$-Flu-dT(pT)$_{14}$	0.49 ± 0.04	0.40 ± 0.03	0.42 ± 0.03	52	54.8 ± 2.5	57.1 ± 2.5	32.9 ± 2.9
dT(pT)$_8$-Flu-dT(pT)$_9$	0.40 ± 0.03	1.00 ± 0.03	0.63 ± 0.03	52	47.6 ± 2.5	48.1 ± 2.3	0 ± 2.3
dT(pT)$_{13}$-Flu-dT(pT)$_4$	0.33 ± 0.03	0.80 ± 0.03	0.54 ± 0.03	52	51.0 ± 2.5	50.5 ± 2.3	15.4 ± 2.5
dT(pT)$_{19}$-Flu-3′	0.37 ± 0.03	0.37 ± 0.03	0.32 ± 0.03	52	59.0 ± 2.8	62.2 ± 3.0	31.9 ± 2.9
5′-Flu-dT(pT)$_9$	0.24 ± 0.03	0.24 ± 0.03	0.17 ± 0.03	52	67.5 ± 3.1	67.6 ± 3.1	47.8 ± 2.9
dT(pT)$_9$-Flu-3′	0.61 ± 0.03	0.61 ± 0.03	0.53 ± 0.03	52	50.7 ± 2.8	47.6 ± 2.9	0 ± 2.3

[a] See the text for details. [b] Average over two measurements using fluorescein or rhodamine as the fluorescence energy transfer acceptor (see the text for details).

Table 2: Fluorescence Energy Transfer Parameters for the Complexes of the Hexameric Helicase RepA Protein of Plasmid RSF1010, Labeled with the Fluorescence Energy Transfer Donor, Coumarin, with Different ssDNA Oligomers, Containing the Fluorescence Energy Transfer Acceptor, Rhodamine, in Buffer T5 (pH 7.6, 10 °C)[a]

ssDNA oligomer	E_D	E_A	E	R_o (Å)	$R(2/3)$ (Å)	$R(2/3)_{av}$ (Å)[b]	x_{av}[b]
5′-Rho-dT(pT)$_{19}$	0.32 ± 0.03	0.08 ± 0.02	0.10 ± 0.02	47	67.4 ± 3.1	65.4 ± 3.1	44.3 ± 3.1
dT(pT)$_3$-Rho-dT(pT)$_{14}$	0.28 ± 0.04	0.14 ± 0.03	0.18 ± 0.03	47	60.5 ± 2.5	57.7 ± 2.5	32.9 ± 2.9
dT(pT)$_8$-Rho-dT(pT)$_9$	0.50 ± 0.03	0.41 ± 0.03	0.45 ± 0.03	47	48.6 ± 2.3	48.1 ± 2.3	0 ± 2.3
dT(pT)$_{13}$-Rho-dT(pT)$_4$	0.54 ± 0.03	0.32 ± 0.03	0.41 ± 0.03	47	50.0 ± 2.3	50.5 ± 2.3	15.4 ± 2.5
dT(pT)$_{19}$-Rho-3′	0.34 ± 0.03	0.09 ± 0.03	0.12 ± 0.03	47	65.3 ± 3.1	62.2 ± 3.0	31.9 ± 2.9
5′-Rho-dT(pT)$_9$	0.25 ± 0.03	0.09 ± 0.03	0.10 ± 0.02	47	67.7 ± 3.1	67.6 ± 3.1	47.8 ± 2.9
dT(pT)$_9$-Rho-3′	0.86 ± 0.03	0.20 ± 0.03	0.58 ± 0.03	47	44.4 ± 2.1	47.6 ± 2.3	0 ± 2.3

[a] See the text for details. [b] Averaged over two measurements using fluorescein or rhodamine as the fluorescence energy transfer acceptor (see the text for details).

the orientation factor, κ^2, is close to the value of $^2/_3$, corresponding to the complete random orientation of the donor absorption and acceptor emission dipoles, respectively (*17*−*19*, *52*, *54*, *56*, *60*) (Materials and Methods). In other words, in such a case, κ^2 does not affect the obtained values of the special separation of the donor and the acceptor. To address this issue, analogous studies, as described above for fluorescein, have been performed using rhodamine as the acceptor. Fluorescence emission spectra of the complexes of RepA-CP with ssDNA oligomers, dT(pT)$_3$-Rho-dT(pT)$_{14}$, the emission spectrum (λ_{ex} = 425 nm) of the RepA-CP complex with dT(pT)$_{19}$, in the absence of the acceptor, and the emission spectrum of dT(pT)$_3$-Rho-dT(pT)$_{14}$, in the complex with the RepA helicase in the absence of the donor, are shown in Figure 5c. The total concentrations of the RepA helicase, RepA-CP, and the labeled and unlabeled ssDNA oligomers are the same as in Figure 5a. As observed for the ssDNA oligomer labeled with fluorescein, the presence of the acceptor (rhodamine) induces a significant quenching of the CP fluorescence, and there is a corresponding increase in the rhodamine fluorescence emission in the presence of the CP.

The normalized emission spectrum of the CP donor, in the complex with rhodamine, and the emission spectrum of rhodamine, in the complex with the donor, are shown in Figure 5d, together with the emission of CP and rhodamine, recorded in the absence of the corresponding fluorescence energy transfer acceptor or donor. The emission intensities of the donor and the acceptor alone and in a complex with the acceptor and the donor, respectively, have been obtained by integrating the corresponding emission spectra (Figure 5d). The degree of binding of the ssDNA oligomers to RepA and RepA-CP and the degree of saturation of the nucleic acid with the helicase are the same as discussed above for the fluorescein-labeled oligomers (*23*). The apparent fluorescence energy transfer efficiencies, E_D and E_A, the Förster fluorescence energy transfer efficiency, E, and the average distance between the donor and the acceptor, $R(2/3)$, have then been obtained using eqs 2, 5, 6, and 8.

The obtained fluorescence energy transfer efficiencies and corresponding average distances, $R(2/3)$, for the entire series of ssDNA oligomers, schematically depicted in Figure 4a, containing rhodamine as the acceptor, are included in Table 2. The behavior of E is very similar to the behavior observed for the ssDNA oligomers containing fluorescein (Table 1). Nevertheless, the values of E are lower than those observed for the fluorescein−CP system, due to the fact that the Förster critical distance (R_o = 47 Å) of the CP−rhodamine donor−acceptor pair is shorter than that (R_o = 52 Å) of the CP−fluorescein pair (Materials and Methods) (*18*). The value of E sharply increases from ∼0.1 for 5′-Rho-dT(pT)$_{19}$ to ∼0.45 for dT(pT)$_8$-Rho-dT(pT)$_9$. The corresponding average distance from the center of mass of the donor to the acceptor, $R(2/3)$, is ∼67.4 Å for 5′-Rho-dT(pT)$_{19}$ and ∼48.6 Å for dT(pT)$_8$-Rho-dT(pT)$_9$ (Table 2). As in the complexes containing fluorescein as the acceptor, a shift of the rhodamine by an additional five nucleotides along the bound ssDNA, i.e., in the complex of the RepA hexamer with dT(pT)$_{13}$-Rho-dT(pT)$_4$, causes, not an increase, but a decrease in the value of E to ∼0.41 and an increase in the average distance [$R(2/3)$] to ∼50 Å. Nevertheless, a further shift of the rhodamine to the 3′ end of the bound DNA in dT(pT)$_{19}$-Rho-3′ is accompanied by a dramatic decrease in the fluorescence energy transfer efficiency E to ∼0.12 and a large increase in the average distance [$R(2/3)$] to ∼65.3 Å. It is evident that both acceptors provide very similar values for the average distances between the donor and acceptor in the RepA hexamer complexes with the ssDNA oligomers, indicating that κ^2 does not affect these measurements. Moreover, the general behavior of the fluorescence energy

transfer efficiency, as a function of the acceptor location on the nucleic acid, for both donor−acceptor systems is also identical (Tables 1 and 2).

Topology of the RepA Total DNA-Binding Site. For a ringlike hexameric structure of the RepA helicase, with the radius of the hexamer being ∼60−80 Å and R_o being 52 Å, the average energy transfer efficiency cannot reach the value of ∼0.54−0.63 if the acceptor is located on the outside of one of the protomers (Figure 3b). However, such high values of E are experimentally observed for the RepA−dT(pT)$_8$-Flu-dT(pT)$_9$ and RepA−dT(pT)$_{13}$-Flu-dT(pT)$_4$ complexes (Table 1). By the same token, when $R_o = 47$ Å, the value of E cannot reach ∼0.41−0.45 which is observed experimentally for the RepA−dT(pT)$_8$-Rho-dT(pT)$_9$ and RepA−dT(pT)$_{13}$-Rho-dT(pT)$_4$ complexes (Table 2). Thus, the high values of the fluorescence energy transfer efficiencies in these complexes provide the first strong evidence that, in the complex of the RepA hexamer, the ssDNA passes through the cross channel of the hexamer (see the Discussion).

Among all examined locations of the acceptor, the highest values of the fluorescence energy transfer efficiency, E, are observed for the ssDNA oligomers with the fluorescein or rhodamine placed in the middle of the nucleic acid molecule, dT(pT)$_8$-Flu-dT(pT)$_9$ and dT(pT)$_8$-Rho-dT(pT)$_9$, respectively (Tables 1 and 2). Slightly lower values of E are observed for dT(pT)$_{13}$-Flu-dT(pT)$_4$ and dT(pT)$_{13}$-Rho-dT(pT)$_4$. Thus, the acceptor, placed at the 10th nucleotide of the nucleic acid molecule (Figure 4a), is closest to the plane with the donor among all examined acceptor locations along the nucleic lattice (Tables 1 and 2). Recall that the donor, CP, is at one of the six possible specific locations on the RepA hexamer, in a plane, which is perpendicular to the side axis of the hexamer (Figure 1a,b). The shortest distance from the donor to fluorescein or rhodamine in dT(pT)$_8$-Flu-dT(pT)$_9$ and dT(pT)$_8$-Rho-dT(pT)$_9$ and the second shortest distance, observed for dT(pT)$_{13}$-Flu-dT(pT)$_4$ and dT(pT)$_{13}$-Rho-dT(pT)$_4$, would only result if the plane with the donor passes the nucleic acid axis around the 10th nucleotide residue of the ssDNA oligomer. In such a structure, fluorescein or rhodamine, attached at the 5′ end of the nucleic acid, would be on one side of the plane with the donor, while fluorescein or rhodamine at the 3′ end would be at opposite sides of the plane with the donor, resulting in the lowest fluorescence energy transfer efficiencies that are also similar to each other, as well as the largest distances for these two locations. This is exactly what is experimentally observed (Tables 1 and 2).

Because the acceptor in complexes of the RepA hexamer with dT(pT)$_8$-Flu-dT(pT)$_9$ and dT(pT)$_8$-Rho-dT(pT)$_9$ is in the plane with the donor and the nucleic acid is bound in the cross channel, the distance from the acceptor to the donor in these complexes is equal to the distance from the donor to the center of the hexamer, q. Averaging over two independent measurements, using fluorescein or rhodamine, provides the relationship $R(2/3) = q = 48.1 \pm 2.3$ Å. This distance is significantly larger than the distance from the cysteine residues to the center of the hexamer (∼35 Å), as suggested by the crystal structure (Figure 1a; see the Discussion). Analogous average distances between the donor and the acceptor, placed at different locations on the ssDNA, averaged over two independent determinations, $R(2/3)_{av}$, are included in Tables 1 and 2. Knowing these averaged

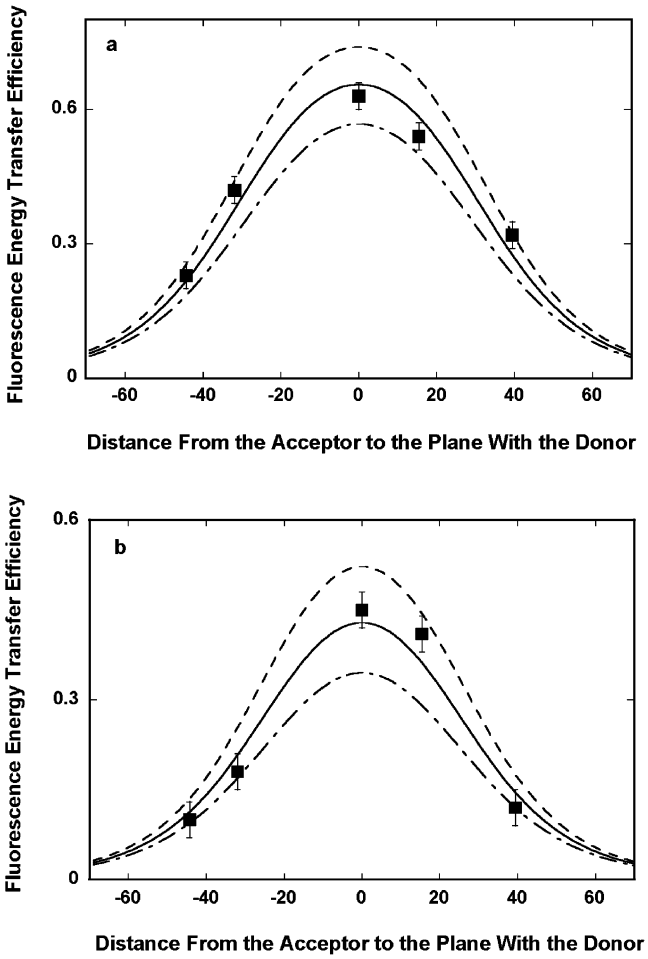

FIGURE 6: (a) Dependence of the average efficiency of Förster fluorescence energy transfer from the donor, CP, on the labeled RepA hexamer, RepA-CP, to the acceptor, fluorescein, placed at different locations on the ssDNA 20-mer, dT(pT)$_{19}$, as a function of the distance from the acceptor to the plane with the donor, x, averaged over two independent measurements of the distances between the donor and the acceptor (Figure 6) (details in the text). The solid line is the nonlinear least-squares fit using eqs 7 and 9 with the distance from the donor to the center of the hexamer, q, as a single fitting parameter and the Förster distance for the CP−fluorescein donor−acceptor pair (R_0) being 52 Å. The plane with the donor, CP, passes the axis of the nucleic acid at the middle of the nucleic acid molecule (details in the text). (b) Dependence of the average efficiency of Förster fluorescence energy transfer from the donor, CP, on the labeled RepA hexamer, RepA-CP, to the acceptor, rhodamine, placed at different locations on the ssDNA 20-mer, dT(pT)$_{19}$, as a function of the distance from the acceptor to the plane with the donor, x, averaged over two independent measurements of the distances between the donor and the acceptor (Figure 6) (details in the text). The solid line is the nonlinear least-squares fit using eqs 7 and 9 with the distance from the donor to the center of the hexamer, q, as a single fitting parameter and the Förster distance for the CP−rhodamine donor−acceptor pair (R_0) being 47 Å. The plane with the donor, CP, passes the axis of the nucleic acid at the middle of the nucleic acid molecule (details in the text).

distances and the average distance from the donor to the center of the hexamer (∼48.1 Å) allows us to obtain the average distances between the acceptor, x, placed in given locations on the DNA, and the plane with the donor, using the Pythagorean formula, defined by eq 9.

The dependence of the experimentally determined fluorescence energy transfer efficiency upon the corresponding distance, x, from the plane with CP, averaged over two

donor−acceptor systems, for fluorescein, placed in different locations along the ssDNA 20-mer, is shown in Figure 6a. The corresponding plot for the nucleic acid labeled with rhodamine is shown in Figure 6b. The plots have a characteristic bell shape with sharp slopes on both sides of the plots, as the acceptor approaches the plane with the donor, with the maximum of the plots centered at the location of the acceptor in the plane with CP (i.e., at $x = 0$). Only the model in which the nucleic acid passes through the cross channel of the hexamer can describe these data. For plotting purposes, we selected the distances from the 5′ end as being negative. However, this selection does not affect the character of the plots. Although the average distance from the donor to the center of the hexamer ($q \sim 48.1$ Å) was used to generate these plots, it does not mean that such an averaged value is the optimal average distance for the specific donor−acceptor pair. The solid lines in panels a and b of Figure 6 are nonlinear least-squares fits of the data, using the distance from CP to the center of the hexamer, q, as a fitting parameter, which provide q values of 46.3 ± 2.4 and 49.3 ± 2.5 Å for fluorescein and rhodamine, respectively. The dashed lines in panels a and b of Figure 6 correspond to the values of q, 3 Å shorter or 3 Å longer than the optimal values of q for a given acceptor−donor pair.

Distances between Different Fluorescence Energy Transfer Acceptors Placed at the 5′ or 3′ Ends of the ssDNA Oligomers, Which Bind Exclusively to the Proper ssDNA-Binding Site of the RepA Helicase and the Donor Located on the RepA Hexamer. When the ssDNA oligomer contains 11 or fewer nucleotides, the nucleic acid exclusively binds to the proper DNA-binding site of the RepA helicase, a specific area within the total DNA-binding site, characterized by the high affinity for the nucleic acid (*23*). To further address the topology of the RepA hexamer−ssDNA complex, we performed fluorescence energy transfer measurements of the distances between the donor, CP, located on the RepA protomer and the acceptor placed at the 5′ or 3′ end of the ssDNA, containing 10 nucleotides (Figure 4b). Binding of the labeled ssDNA 11-mers to the RepA hexamer is characterized by the same binding constant [$K_{10} = (3.1 \pm 0.4) \times 10^6$ M^{-1}] as the binding of the unmodified dT(pT)$_{10}$, indicating the labeling does not affect the energetics of the enzyme−ssDNA interactions (data not shown) (*23*).

Fluorescence emission spectra ($\lambda_{ex} = 425$ nm) of the complex of RepA-CP with the ssDNA 11-mer, dT(pT)$_9$-Flu-3′, the emission spectrum of the RepA-CP complex with dT-(pT)$_{10}$, in the absence of the acceptor, and the emission spectrum of dT(pT)$_9$-Flu-3′ in the complex with the RepA helicase, in the absence of the donor, are shown in Figure 7a. The total concentrations of the RepA helicase and RepA-CP are 1×10^{-6} M. The total concentrations of the labeled and unlabeled ssDNA oligomer are 1×10^{-6} M. The spectra in Figure 7a show that the presence of the acceptor (fluorescein) induces a significant quenching of the donor fluorescence. Correspondingly, there is a significant increase in the acceptor fluorescence emission in the presence of the donor. The normalized emission spectrum of the CP donor in the complex with the acceptor and the emission spectrum of the fluorescein acceptor in the complex with the donor are shown in Figure 7b, together with the emission of the donor and acceptor, recorded in the absence of the corresponding fluorescence energy partner. These spectra were obtained in a manner analogous to that described for the RepA−ssDNA 20-mer complexes (Figure 5b,d). Subsequently, the emission intensities of the donor and the acceptor alone and in the complex with the corresponding fluorescence energy transfer partner have been obtained by integrating the emission spectra in Figure 7b. At the selected equal total concentrations of the enzyme and the 11-mer, the degree of binding of the ssDNA 11-mer to RepA and RepA-CP (ν_D) and the degree of saturation of the DNA with the helicase (ν_A) are both ≈0.57. The apparent fluorescence energy transfer efficiencies, E_D and E_A, the Förster fluorescence energy transfer efficiency, E, and the average distance between the donor and acceptor, $R(2/3)$, have been obtained using eqs 2, 5, 6, and 8. Analogous sets of fluorescence emission spectra ($\lambda_{ex} = 425$ nm) of the complex of RepA-CP with the ssDNA 11-mer, dT(pT)$_9$-Rho-3′, containing rhodamine as the acceptor, are shown in panels c and d of Figure 7.

The same fluorescence energy transfer experiments have been performed for the ssDNA 11-mers, containing fluorescein and rhodamine at the 5′ end, 5′-Flu-dT(pT)$_9$ and 5′-Rho-dT(pT)$_9$, respectively (data not shown). The obtained fluorescence energy transfer efficiencies and the corresponding average distances for all examined ssDNA 11-mers are included in Tables 1 and 2. The difference between the values of the fluorescence energy transfer, E, between the ssDNA 11-mers, containing the acceptor at the 5′ end, as compared to the ssDNA 11-mers, containing the acceptor at the 3′ end, is dramatic. For 5′-Flu-dT(pT)$_9$ and 5′-Rho-dT(pT)$_9$, the values of E are only ∼0.17 and ∼0.1, respectively. For dT-(pT)$_9$-Flu-3′ and dT(pT)$_9$-Rho-3′, these values are ∼0.53 and ∼0.58, respectively. The corresponding average distances from the center of mass of the acceptor to the donor, $R(2/3)$, are ∼67.5 and ∼50.7 Å for 5′-Flu-dT(pT)$_9$ and dT(pT)$_9$-Flu-3′, respectively. The same distances for 5′-Rho-dT(pT)$_9$ and dT(pT)$_9$-Rho-3′ are ∼67.7 and ∼44.4 Å, respectively. Thus, both different donor−acceptor pairs provide very similar distances between the 5′ and 3′ ends of the bound ssDNA 11-mer and the donor on the RepA hexamer, which is empirical evidence that the value of the orientation factor, κ^2, is close to a value of $^2/_3$, corresponding to the complete random orientation of the donor absorption and acceptor emission dipoles, respectively (Materials and Methods) (*17*−*19*, *54*, *60*). The distances from the 5′ and 3′ ends of the bound ssDNA 11-mer, averaged over the two examined donor−acceptor pairs, are ∼67.6 and ∼47.6 Å, respectively. Notice, these distances are, within experimental accuracy, identical to the corresponding averaged distances obtained for the ssDNA 20-mers, with the acceptors located at the 5′ end or in the middle of the nucleic acid (Tables 1 and 2). This distance similarity shows that the ssDNA 11-mer, bound in the proper DNA-binding site of the RepA helicase, is in the same location as the 5′ end side of the bound ssDNA 20-mer, which encompasses the total DNA-binding site of the enzyme (see the Discussion).

Global Conformation of the RepA Hexamer in Solution. Both chemical labeling and fluorescence energy transfer measurements indicate that the structure of the RepA hexamer is different from the structure determined in crystallographic studies (see above). Analytical sedimentation provides direct and unique information about the global conformation of a macromolecule (*43*, *44*). The sedimenta-

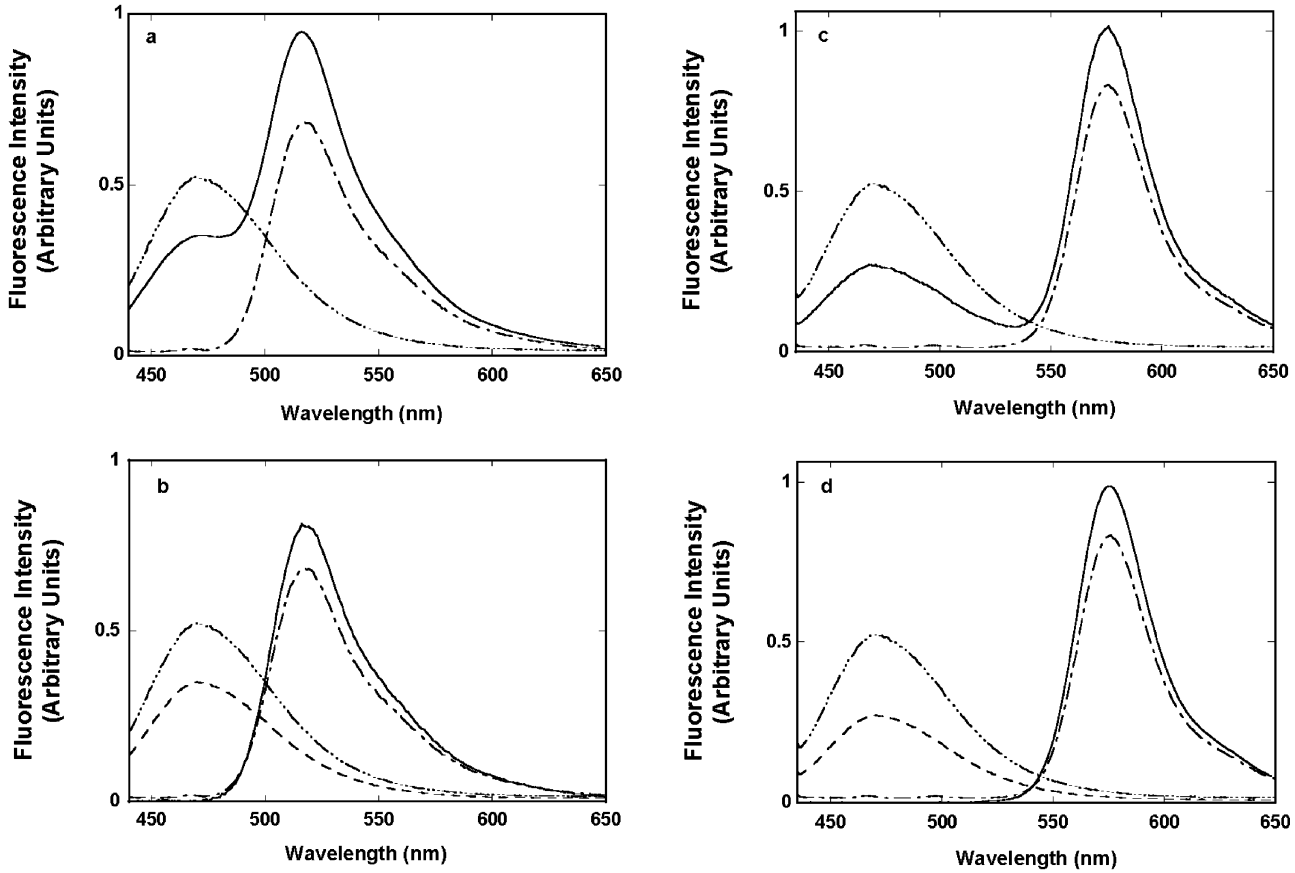

FIGURE 7: (a) Fluorescence emission spectrum ($\lambda_{ex} = 425$ nm) of the RepA hexamer, RepACP, labeled with the coumarin derivative, CP, in the presence of unlabeled dT(pT)10 (—···—), fluorescence emission spectrum of the ssDNA oligomer, dT(pT)$_9$-Flu-3′, in the presence of the unlabeled RepA hexamer (— - —), and fluorescence emission spectrum of the labeled RepA hexamer, RepA-CP, in the presence of the labeled ssDNA oligomer, dT(pT)$_9$-Flu-3′ (—), in buffer T5 (pH 7.6, 10 °C) containing 1 mM $MgCl_2$, 10 mM NaCl, 0.5 mM AMP-PNP, and 10% glycerol. Concentrations of RepA-CP and the ssDNA oligomer are 1×10^{-6} M (hexamer) and 1×10^{-6} M (oligomer), respectively (details in the text). (b) Fluorescence emission spectrum ($\lambda_{ex} = 425$ nm) of the labeled RepA hexamer, RepA-CP, in the presence of the unlabeled dT(pT)$_{10}$ (—···—), fluorescence emission spectrum of RepA-CP normalized to the emission of RepA-CP in a complex with dT(pT)$_9$-Flu-3′ (- - -), fluorescence emission spectrum of dT(pT)$_9$-Flu-3′ in the presence of the unlabeled RepA hexamer (— - —), and fluorescence emission spectrum of dT(pT)$_9$-Flu-3′ in a complex with RepA-CP, after subtraction of the normalized spectrum of RepA-CP in the same complex (—). Solution conditions and concentrations of RepA-CP and the ssDNA oligomer are the same as those described for panel a (details in the text). (c) Fluorescence emission spectrum ($\lambda_{ex} = 425$ nm) of the RepA hexamer, labeled with coumarin, CP, RepA-CP, in the presence of unlabeled dT(pT)$_{10}$ (—···—), fluorescence emission spectrum of the ssDNA oligomer, dT(pT)$_9$-Rho-3′, in the presence of the unlabeled RepA hexamer (— - —), and fluorescence emission spectrum of the labeled RepA hexamer, RepA-CP, in the presence of the labeled ssDNA oligomer, dT(pT)$_9$-Rho-3′ (—), in buffer T5 (pH 7.6, 10 °C) containing 1 mM $MgCl_2$, 10 mM NaC1, 0.5 mM AMP-PNP, and 10% glycerol. Concentrations of RepA-CP and the ssDNA oligomer are 1×10^{-6} M (hexamer) and 1×10^{-6} M (oligomer), respectively (details in the text). (d) Fluorescence emission spectrum ($\lambda_{ex} = 425$ nm) of the labeled RepA hexamer, RepA-CP, in the presence of unlabeled dT(pT)$_{10}$ (—···—), fluorescence emission spectrum of RepA-CP normalized to the emission of RepA-CP in a complex with dT(pT)$_9$-Rho-3′ (- - -), fluorescence emission spectrum of dT(pT)$_9$-Rho-3′ in the presence of the unlabeled RepA hexamer (— - —), and fluorescence emission spectrum of dT(pT)$_9$-Rho-3′ in a complex with RepA-CP, after subtraction of the normalized spectrum of RepA-CP in the same complex (—). Solution conditions and concentrations of RepA-CP and the ssDNA oligomer are the same as those described for panel c (details in the text).

tion velocity profiles (monitored at 280 nm) of the free RepA helicase, in buffer T5 (pH 7.6, 10 °C), are shown in Figure 8a. Inspection of the profiles clearly shows that there is a single moving boundary, indicating the presence of a single molecular species. The sedimentation coefficient of the protein, $s_{20,w}$, has been obtained using the time derivative approach, which provides a value for $s_{20,w}$ of 8.4 ± 0.09. The partial specific volume ($\bar{\nu}$) of the RepA hexamer, calculated on the basis of the amino acid composition, is 0.736 mL^{-1} g^{-1}, and the average degree of hydration (h) is 0.3 g of H_2O/g of protein) (*61*, *62*). Modeling the RepA hexamer as an oblate ellipsoid of revolution and using the Perrin formula for friction coefficient of the ellipsoid provide, for this value of $s_{20,w}$, the axial ratio of the RepA hexamer, $p = 4.5 \pm 0.6$ (*41*, *45*, *46*). This is an axial ratio significantly larger than the value of ~2.3 for the RepA hexamer in the crystal (Figure 1a,b). The sedimentation velocity profiles (monitored at 295 nm) of the RepA helicase in the presence of AMP-PNP, in buffer T5 (pH 7.6, 10 °C), are shown in Figure 8b. The concentration of AMP-PNP is 1×10^{-5} M. The profiles also show a single moving boundary, indicating the presence of a single molecular species. However, the profiles are characterized by the sedimentation coefficient ($s_{20,w} = 7.6 \pm 0.1$), which is much lower than the value observed for the free hexamer. Parallel equilibrium sedimentation studies showed that the molecular weight of the hexamer is not affected by the cofactor (data not shown). Analysis using the Perrin formula, with the same values of the partial specific volume and the degree of hydration as for the free protein, provide the axial ratio $p = 1 \pm 0.2$ (*41*,

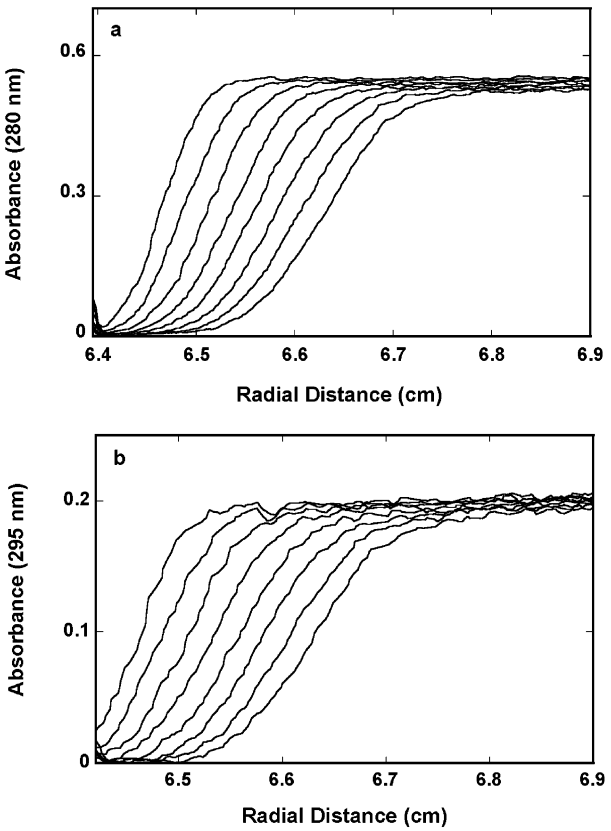

FIGURE 8: (a) Sedimentation velocity profiles (monitored at 280 nm) of the RepA helicase alone, in buffer T5 (pH 7.6, 10 °C). The concentration of the protein is 6×10^{-6} M (hexamer), with a time interval of 14 min at 35 000 rpm. (b) Sedimentation velocity profiles (monitored at 295 nm) of the RepA helicase−AMP-PNP complex, in buffer T5 (pH 7.6, 10 °C). The concentrations of the protein and the nucleotide cofactor are 6×10^{-6} M (hexamer) and 6×10^{-6} M, respectively, with a time interval of 14 min at 35 000 rpm (Materials and Methods).

45, *46*). Independent of the approximate nature of these calculations, both values of the sedimentation coefficients indicate that the global structure of the RepA hexamer, in solution, is different from the crystal structure and is strongly affected by the presence of the nucleotide cofactor (see the Discussion).

DISCUSSION

In the Equilibrium Complex with the RepA Hexamer, the ssDNA Passes through the Cross Channel of the Ringlike Structure of the Enzyme. Elucidation of the fundamental aspects of the structure of a hexameric helicase complex with the ssDNA in solution is of paramount importance for understanding the mechanism of enzyme activities (*3*−*5*, *17*, *18*, *24*−*28*). In the case of a handful of currently well-studied hexameric helicases, the nucleic acid crosses the inner channel of the ringlike hexameric structure (*24*−*28*). However, the issue of the mode of binding of a nucleic acid to a hexameric helicase is more complex than what may be assumed from these known cases. For instance, different behavior seems to occur in the case of the *E. coli* transcription termination factor, Rho helicase, where binding of the nucleic acid, in both inside and outside modes, has been proposed and the presence of different sets of nucleic acid-binding sites inferred (*29*−*32*). The cross channel of the DnaB hexamer has a diameter of ∼40 Å, which can accommodate the ssDNA strand or the dsDNA helix (*33*, *34*). The RepA protein is the smallest known helicase, and the diameter of the cross channel is only ∼17 Å in the crystal structure of the enzyme (*10*). The hexameric structure of the RepA protein is unusually stable, and the stability is not affected by nucleotide cofactors or nucleic acid. The DnaB protein forms a stable hexamer. However, the integrity of the DnaB hexamer is controlled by specific magnesium binding (*12*). Kinetic studies indicate the DnaB helicase must possess outside nucleic acid-binding site(s), but in the stationary complex, the equilibrium is very strongly shifted toward the complex with the nucleic acid inside the cross channel (*36*, *63*, *64*). Whether this equilibrium is shifted in all hexameric helicases to the same extent as in the DnaB helicase, in particular, in the case of hexameric helicases, which are as stable as the RepA hexamer, is unknown.

Fluorescence energy transfer from a donor to an acceptor is one of the most intensively used methods in studying macromolecular distances, in solution, and is one of the major methods used to examine the structure and function of large protein−nucleic acid complexes (*65*−*69*). A striking result of the fluorescence energy transfer measurements described in this work is the high value of the efficiency of fluorescence energy transfer ($E = 0.63 \pm 3$) from the donor, CP, located at one of the cysteine residues of the hexamer, to fluorescein as the fluorescence energy transfer acceptor placed in the middle of the bound ssDNA 20-mer, which encompasses the total DNA-binding site of the enzyme (Figure 4a and Tables 1 and 2). The values of E for the fluorescein placed five nucleotides from the 5′ and 3′ ends of the nucleic acid are 0.42 ± 0.03 and 0.54 ± 0.03, respectively. The value of E for the ssDNA-11-mer, dT(pT)$_9$-Flu-3′, bound in the proper DNA-binding site is 0.53 ± 0.03. The theoretical analysis of the energy transfer process for two possible modes of binding of ssDNA to the RepA hexamer shows that with the radius of the hexamer ($b \approx 60$ Å) and the Förster critical distance ($R_o = 52$ Å) the efficiency of fluorescence energy transfer from the CP to the fluorescein cannot exceed the value of ∼0.34 for the binding mode, in which the ssDNA is bound on the outside of the hexamer (Figure 3b). Only when the DNA is placed in the center of the hexamer can the energy transfer efficiency reach the experimentally observed values for the RepA−ssDNA complex.

The same theoretical analysis for the fluorescence energy transfer donor−acceptor pair characterized by a b of 60 Å and an R_o of 47 Å, corresponding to the examined CP−rhodamine donor−acceptor pair, shows that the average fluorescence energy transfer efficiency, E, cannot exceed the value of ∼0.3, even under the most favorable conditions when the acceptor is in the same plane with the donor and when the nucleic acid is bound on the outside of the RepA hexamer (data not shown). Yet, the experimentally determined values of E for dT(pT)$_8$-Rho-dT(dT)$_9$ and dT(pT)$_{13}$-Rho-dT(dT)$_4$ are 0.45 ± 0.03 and 0.41 ± 0.03, respectively. Correspondingly, an E value of 0.58 ± 0.03 has been obtained for the ssDNA 11-mer, dT(pT)$_9$-Rho-3′, bound to the proper DNA-binding site of the enzyme. These values of E are much higher than the physically possible value for the outside mode of DNA binding (Table 2). Therefore, the observed high-energy transfer efficiency for four independent fluorescence energy transfer donor−acceptor systems can occur only if the acceptor is a similar distance from each of

the donors in the donor ring, i.e., when the ssDNA is bound in the cross channel of the hexamer.

The Bound DNA Assumes Heterogeneous Structure Reflecting the Heterogeneous Structure of the Total DNA-Binding Site of the RepA Hexamer. Fluorescence energy transfer experiments, with the acceptor located along the bound ssDNA oligomer, fully support the model of the hexamer−ssDNA complex in which DNA passes through the inner channel of the hexamer and provide additional information about the structure of the complex. The highest fluorescence energy transfer efficiency is observed in the case of $dT(pT)_8$-Flu-$dT(dT)_9$ and $dT(pT)_8$-Rho-$dT(dT)_9$ with E values of ≈0.63 and ≈0.45, respectively, i.e., for the acceptor located in the middle of the ssDNA oligomer (Figure 4a). On the other hand, shifting the location of the acceptor by the same distance of five nucleotides from both sides of the ssDNA molecule results in a large decrease in the energy transfer efficiency, while a further dramatic decrease in E is observed for the acceptors located at the 5′ and 3′ ends of the bound nucleic acid (Tables 1 and 2 and Figure 4). Theoretical analysis of the energy transfer process indicates that such a large decrease in E is predicted by the model in which the ssDNA binds in the cross channel of the hexamer, but not by the outside binding mode (Figure 3a,b).

The largest values of E obtained for $dT(pT)_8$-Flu-$dT(dT)_9$ and $dT(pT)_8$-Rho-$dT(dT)_9$ oligomers indicate that the plane with the donor passes the nucleic acid axis around the 10th nucleotide from the 5′ or 3′ end. In other words, in the complex, the bound ssDNA oligomer protrudes approximately 10 nucleotides above and below the plane containing six cysteine residues of the RepA hexamer, where the donor, CP, is located (Figure 1a,b). Because the plane with the cysteine residues is located only ∼12 Å from one end of the RepA hexamer in the large domain of the enzyme, such a symmetric location of the bound ssDNA oligomer, with respect to the plane with the cysteine residues, suggests that only a part, ∼16−17 nucleotides, of the bound nucleic acid is directly engaged in interactions with the enzyme. This value is slightly lower than the site size of 19 ± 1 nucleotides of the RepA hexamer−ssDNA complex obtained in the thermodynamic studies of binding of the protein to the nucleic acid (*23*). This should not be surprising, as the thermodynamic data provide the value of the site size, directly reflecting the length of the ssDNA fragment required for the second hexamer to associate with the DNA next to another bound hexamer, while the fluorescence energy transfer data reflect the binding to an isolated ssDNA oligomer (*23*).

The data for the average distance from the acceptor to the plane with the donor, shown in panels a and b of Figure 6, provide crucial information about the structure of the bound nucleic acid, which encompasses the total DNA-binding site of the enzyme. Recall that the average distance between the 5′ and 3′ ends of the labeled ssDNA oligomers, in solution, is ∼75 Å (see above) (*18*). Thus, the length of the free nucleic acid is very similar to the length of the corresponding single strand of the dsDNA in the B form (∼78 Å) (*58*, *59*). The end-to-end distance of the bound ssDNA to the RepA hexamer is ∼83 Å (Figure 6a,b). Thus, the nucleic acid bound to the total DNA-binding site of the RepA helicase assumes an extended conformation in the complex with helicase, which is different from the B form of the dsDNA. The obtained average distance from the acceptor in $dT(pT)_{13}$-Flu-$dT(pT)_4$ and $dT(pT)_{13}$-Rho-$dT(pT)_4$, to the plane with the donor, is ∼15.4 Å. For the acceptor placed an additional six nucleotides further, at the 3′ end in $dT(pT)_{19}$-Flu-3′ and $dT(pT)_{19}$-Rho-3′, the obtained distance to the plane with the donor is ∼39 Å. Recall that the acceptor residue at the 3′ end contributes the same length as an additional base. Thus, the increments of the distance per each additional base, from the plane with the donor to the 3′ end of the bound nucleic acid, are ∼3.1 and ∼3.9 Å for the two considered segments of the nucleic acid and are similar to the increment of ∼3.54 Å of the single strand of the dsDNA in the B form (*58*, *59*).

The situation is very different for the part of the bound DNA from its 5′ end side. The obtained average distance from the acceptor in $dT(pT)_3$-Flu-$dT(pT)_{14}$ and $dT(pT)_3$-Rho-$dT(pT)_{14}$, to the plane with the donor, is ∼32 Å, much larger than the distance of ∼15.4 Å. For the acceptor placed an additional six nucleotides further, at the 5′ end, in 5′-Flu-$dT(pT)_{19}$ and 5′-Rho-$dT(pT)_{19}$, the obtained average distance to the plane with the donor is ∼44 Å. Thus, the increments of the distance per each additional base from the plane with the donor, for these two segments of the bound DNA, are ∼6.4 and ∼2 Å, respectively. First, both these values are very different from the increment of ∼3.54 Å for the single strand of dsDNA in the B form. Second, they are very different from each other. The first five nucleotides from the plane with the donor, on the 5′ end of the bound DNA, are in a very extended conformation, with the average distance between bases reaching ∼6.4 Å. The six remaining nucleotides, toward the 5′ end of the nucleic acid, either are in a much more compressed conformation than the single strand of the dsDNA in the B form or are tightly coiled, as the nucleic acid exits the total DNA-binding site. These data clearly indicate the presence of regions in the total DNA-binding site of the RepA hexamer which, locally, very differently affect the structure of the bound nucleic acid, i.e., the heterogeneous structure of the total binding site (*23*). Heterogeneous structures of the total DNA-binding site have been found for the *E. coli* DnaB hexamer as well as for the monomeric *E. coli* PriA helicase (*17*, *70*, *71*). The heterogeneous structure of the ssDNA bound to the RepA helicase, obtained in this work, strongly and directly supports the findings that the total DNA-binding sites of the helicases have a complex structure and locally exert dramatically different effects on the conformational states of the bound nucleic acid.

The Proper DNA-Binding Site of the RepA Hexamer Exerts a Major Effect on the Conformation of the Bound ssDNA. Quantitative thermodynamic studies of the binding of ssDNA to the RepA helicase provided the first indication that the total DNA-binding site of the RepA helicase has a heterogeneous structure and contains an area, the proper DNA-binding site, which has strong ssDNA affinity and encompasses up to ∼11 nucleotides of the total 19 ± 1 nucleotides of the total DNA-binding site. Moreover, the data also indicate that the proper DNA-binding site is located in the central part of the RepA hexamer (*23*). The 3′ end of the bound 11-mer in the proper DNA-binding site is virtually the same distance, ∼48 Å, from the donor, CP, as the middle nucleotide of the 20-mer, which encompasses the total site (Tables 1 and 2). The 5′ end of the bound 11-mer is the

same distance from the donor as the 5′ end of the 20-mer and much farther from the plane with the donor, at an average distance of ∼67.6 Å. Having these two distances from the plane with the donor, we can estimate, using eq 9, the length of the bound 11-mer to be ∼48 Å, which provides the average separation between the adjacent bases of ∼4.3 Å, in the bound 11-mer. This value is equal to the average of the base separations of two segments of the bound 20-mer from its 5′ end side (see above).

First, these results independently indicate that the conformation of the bound ssDNA, in the proper DNA-binding site of the RepA helicase, is strongly stretched as compared to the conformation of the corresponding ssDNA strand of the dsDNA in the B form. Second, they also provide independent support for the finding of the heterogeneous structure of the RepA helicase. Notice that if the entire labeled 20-mer bound to the total DNA-binding were stretched to the same extent as the ssDNA in the proper site, then the distance between the 5′ and 3′ ends would be ∼96 Å, not ∼83 Å, as experimentally observed (see above). Furthermore, the profound differences in the local DNA structure of the nucleic acid bound to the RepA helicase provide a clue about the experimentally observed dramatic difference in the thermodynamic response of the proper DNA-binding site to the changes in the solution conditions, as compared to the analogous response of the total site. While the binding of the DNA to the proper DNA-binding site is accompanied by net ion uptake, binding to the total DNA-binding site is accompanied by net ion release (*23*). In other words, ion binding is necessary to stabilize the stretched conformation of the ssDNA in the proper site, while it strongly destabilizes interactions of the ssDNA, in the more relaxed conformation with the enzyme outside the proper site.

The RepA Hexamer Binds the ssDNA in a Strictly Single Orientation with Respect to the Sugar−Phosphate Backbone of the Nucleic Acid. The apparent symmetric location of the bound ssDNA oligomer in the total DNA-binding site of the enzyme, with respect to the plane containing the cysteine residues, may seem to prevent the determination of the orientation of the RepA hexamer on the ssDNA lattice. However, the asymmetric changes in the structure of the bound ssDNA provide a clear clue. The structure of the 10-nucleotide segment of the bound DNA, from the plane of the donor to the 3′ end of the nucleic acid, is similar to the structure of the single strand of the dsDNA; i.e., it is similar to the structure of the free $dT(pT)_{19}$ in solution. In other words, the structure of this fragment is only slightly affected by the binding to the enzyme (see above). On the other hand, the structure of the remaining 10-nucleotide segment from the plane with the donor to the 5′ end of the bound DNA is dramatically changed in the complex with the helicase. These data strongly indicate that the entire segment of the bound ssDNA, from the 5′ end of the nucleic acid, is directly engaged in interactions with the helicase; i.e., it is placed directly in the cross channel. Because the plane with the six cysteine residues and the donor, CP, is in the large domain and only ∼12 Å from the end of the RepA molecule, such a dramatically different effect of the enzyme on the bound DNA structure can only happen if the hexamer is predominantly oriented with the large domain toward the 3′ end of the bound nucleic acid.

Results on the structure and location of the 11-mer, exclusively bound to the proper DNA-binding site, provide additional strong evidence of a single orientation of the enzyme in the complex with the ssDNA. The average fluorescence energy transfer efficiencies and corresponding distances between the 5′ and 3′ ends of the ssDNA 11-mer, bound in the proper DNA-binding site, are virtually identical to the corresponding parameters obtained for the 5′ end and the middle nucleotide of the bound 21-mer (Tables 1 and 2). The symmetry of the RepA−20-mer complex is not present in the complex with the 11-mer, and the 5′ end of the 11-mer is clearly much farther, approximately 48 Å, from the plane with the donor, CP, than its 3′ end. Moreover, both the 5′ side of the bound 20-mer and the entire 11-mer have extended conformations, reflecting the interactions with the proper DNA-binding site. Because the 11-mer is exclusively bound to the proper DNA-binding site, located in the central part of the total DNA-binding site, these data indicate that the 5′ side of the 20-mer, which encompasses the total DNA-binding site, is also exclusively engaged in interactions with the proper site, i.e., with the central part of the total DNA-binding site of the enzyme.

The dramatic difference in the conformational changes in the bound DNA, at the 5′ end side as compared to the 3′ end side of the nucleic acid, induced by the RepA hexamer, the dramatic differences between the distances from the 5′ and 3′ end to the donor, and the effect of the enzyme on the structure of the ssDNA 11-mer, bound exclusively to the centrally located proper DNA-binding site, provide clear evidence that the RepA hexamer assumes a strictly single orientation, with respect to the sugar−phosphate backbone of the bound ssDNA. Notice that it has been determined that the *E. coli* hexameric DnaB helicase also assumes a strictly single orientation on the bound DNA, facing the 3′ end of the nucleic acid with its large 33 kDa domain (*17*−*19*). Thus, both RepA and the DnaB helicase have the same strictly single orientation on the ssDNA, indicating that this may be the general behavior of hexameric helicases.

The orientation of the RepA hexamer in the complex with the ssDNA and the schematic structure of the nucleic acid in the complex are depicted in Figure 9. The enzyme binds the ssDNA with the total site size of 19 ± 1 nucleotides. The large domain of the enzyme, containing the cysteine residues, is directed toward the 3′ end of the nucleic acid. The total DNA-binding site, located in the cross channel, has a heterogeneous structure. The DNA is strongly stretched in the central part of the cross channel, corresponding to the location of the proper DNA-binding site. The small ovals indicate the presumed location of the ATP-binding sites. Notice that the obtained data indicate that the ssDNA is not an impartial partner in the helicase−ssDNA complex, which serves as a "neutral track" on which the enzyme performs the mechanical translocation, which is the current line of thinking. The ssDNA undergoes large and localized conformational changes in the heterogeneous binding site of the enzyme. In fact, the obtained results suggest that the energy stored in the ssDNA may be part of the energy used to propel the enzyme along the nucleic acid lattice.

The Structure of the RepA Hexamer in Solution Differs Significantly from the Crystal Structure of the Enzyme, Indicating Significant Conformational Flexibility of the Enzyme. As we pointed out above, the fact that only ∼0.31

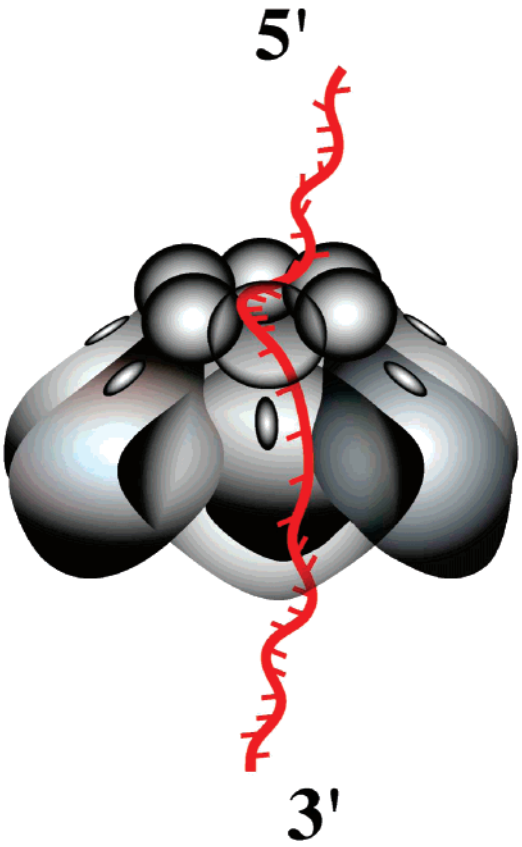

FIGURE 9: Schematic structure of the RepA hexamer bound in a stationary complex to the ssDNA, based on the results obtained in this work. The ssDNA passes the cross channel of the RepA hexamer. In the complex, the helicase assumes a strictly single orientation with respect to the sugar−phosphate backbone of the nucleic acid with the small domain of each protomer oriented toward the 5′ end and the large domain oriented toward the 3′ end of the bound DNA. The cross channel constitutes the total DNA binding of the enzyme (*23*). The bound ssDNA in the proper DNA-binding site, which is located in the central part of the total DNA-binding site, is profoundly affected by the interactions with the helicase with regions of stretch and compressed structure. The structure of the segment of the nucleic acid from its 3′ end, which is leaving the cross channel of the hexamer, is not affected by the helicase and has a conformation similar to the conformation of the free ssDNA in solution. The arrow indicates the 5′ → 3′ direction of the mechanical translocation of the enzyme along the DNA lattice and the unwinding reaction.

CP per RepA hexamer can be introduced in specific chemical labeling of the six cysteine residues of the hexamer has provided the first indication that the structure of the RepA hexamer in solution is different from the crystal structure of the protein (*10*). It indicates that the cysteines are only partially accessible to the chemical labeling, although the crystal structure suggests rather easy solvent access. However, the major additional evidence that the solution structure of the hexamer is different from its crystal structure comes directly from the distance measurement and hydrodynamic data. In the crystal structure, the distance from each cysteine residues to the center of the hexamer is ∼35 Å (Figure 1a,b). On the other hand, the experiments, using different donor−acceptor pairs and different nucleic acids, bound in different locations, show that, in solution, the same average distance from the center of the hexamer and the cysteine residues is ∼48 Å (Tables 1 and 2). Moreover, the distance from the 5′ end of the bound 20- or 11-mer to the plane with the cysteine residues is significantly larger than the length of the side axis of the RepA hexamer, parallel to the axis of the cross channel (Figure 1b).

There are two important consequences of this result. First, as we previously pointed out, different donor−acceptor pairs give very similar distances, and this fact eliminates any substantial effect of the orientation factor, κ^2, on these measurements (*18*, *54*) (see above). Thus, these data show that the dimensions of the RepA hexamer, in the tertiary complex with the nucleotide cofactor (AMP-PNP) and the ssDNA, are significantly larger than the dimensions of the RepA hexamer indicated by the crystal structure (*10*). Notice that the crystal structure of the hexamer has been determined for the protein dodecamer, where interactions between the hexamers may require a specific conformation of both RepA hexamers. Second, these data also strongly suggest that the diameter of the cross channel of the RepA hexamer is significantly larger than the value of ∼17 Å in the crystal structure. The analytical ultracentrifugation results fully corroborate the conclusion that the RepA hexamer assumes a structure in solution different from that observed in the crystal form. Moreover, these results also indicate the global structure of the hexamer is under control of the nucleotide cofactor binding (Figure 8a,b).

Altogether, for the first time, these results strongly indicate that the exceptionally stable RepA hexamer is a surprisingly dynamic entity, which can assume different conformations, in solution, with the crystal structure being only one of them. Although the exact mechanism of binding of the RepA hexamer to the ssDNA is still unknown, the fact that the DNA is bound in the inner channel of the hexamer in the presence of an ATP nonhydrolyzable analogue, AMP-PNP, and the hexamer is the entity which binds the ssDNA indicates that such a mechanism must include a conformational change, which leads to a transient opening of the hexamer, in the absence of ATP hydrolysis. Such a mechanism has indeed been found in the case of another stable hexameric helicase, the *E. coli* DnaB protein (*36*). The necessary conformational changes must involve large reorientations of the hexamer subunits, which are already indicated by the fluorescence energy transfer data described above. The conformational flexibility of the RepA hexamer and the response of the structure of the protein to the binding of nucleotide cofactors and the DNA are currently being addressed in our laboratory.

ACKNOWLEDGMENT

We thank Gloria Bellard for reading the manuscript.

REFERENCES

1. Kornberg, A., and Baker, T. A. (1992) *DNA Replication*, pp 275−306, Freeman, San Francisco.
2. Marians, K. J. (1992) Prokaryotic DNA Replication, *Annu. Rev. Biochem. 61*, 673−719.
3. Lohman, T. M., and Bjornson, K. P. (1996) Mechanisms of Helicase-Catalyzed DNA Unwinding, *Annu. Rev. Biochem. 65*, 169−214.
4. von Hippel, P. H., and Delagoutte, E. (2003) Helicase Mechanisms and the Coupling of Helicases Within Macromolecular Machines. Part I: Structures and Properties of Isolated Helicases, *Q. Rev. Biophys. 35*, 431−478.
5. von Hippel, P. H., and Delagoutte, E. (2003) Helicase Mechanisms and the Coupling of Helicases Within Macromolecular Machines. Part II: Integration of Helicases Into Cellular Processes, *Q. Rev. Biophys. 36*, 1−69.

6. De Gaaf, J., Crossa, J. H., Heffron, F., and Falkow, S. (1978) Replication of the Nonconjugative Plasmid RSF1010 in *Escherichia coli* K-12, *J. Bacteriol. 134*, 1117−1122.
7. Guerry, P., van Embden, J., and Falkow, S. (1974) Molecular Nature of Two Nonconjugative Plasmids Carrying Drug Resistance Genes, *J. Bacteriol. 117*, 987−997.
8. Scherzinger, E., Ziegelin, G., Barcena, M., Carazo, J. M., Lurz, R., and Lanka, E. (1997) The RepA Protein of Plasmid RSF1010 Is a Replicative DNA Helicase, *J. Biol. Chem. 272*, 30228−30236.
9. Roleke, D., Hoier, H., Bartsch, C., Umbach, P., Scherzinger, E., Lurz, R., and Saenger, W. (1997) Crystallization and Preliminary Crystallographic and Electron Microscopy Study of Bacterial DNA Helicase (RSF1010 RepA), *Acta Crystallogr. D53*, 213−216.
10. Niedenzu, T., Roleke, D., Bains, G., Scherzinger, E., and Saenger, W. (2001) Crystal Structure of the Hexameric Helicase RepA of Plasmid RSF1010, *J. Mol. Biol. 306*, 479−487.
11. Xu, H., Frank, J., Holzwarth, J. F., Saenger, W., and Behlke, J. (2000) Interaction of different oligomeric states of hexameric DNA-helicase RepA with single-stranded DNA studied by analytical ultracentrifugation, *FEBS Lett. 482*, 180−184.
12. Bujalowski, W., Klonowska, M. M., and Jezewska, M. J. (1994) Oligomeric Structure of *Escherichia coli* Primary Replicative Helicase DnaB Protein, *J. Biol. Chem. 269*, 31350−31358.
13. Jezewska, M. J., Rajendran, S., and Bujalowski, W. (1998) Complex of *Escherichia coli* Primary Replicative Helicase DnaB Protein with a Replication Fork. Recognition and Structure, *Biochemistry 37*, 3116−3136.
14. Bujalowski, W., and Jezewska, M. J. (1995) Interactions of *Escherichia coli* Primary Replicative Helicase DnaB Protein with Single-Stranded DNA. The Nucleic Acid Does Not Wrap Around the Protein Hexamer, *Biochemistry 34*, 8513−8519.
15. Jezewska, M. J., Kim, U.-S., and Bujalowski, W. (1996) Binding of *Escherichia coli* Primary Replicative Helicase DnaB Protein to Single-Stranded DNA. Long-Range Allosteric Conformational Changes within the Protein Hexamer, *Biochemistry 35*, 2129−2145.
16. Jezewska, M. J., Rajendran, S., and Bujalowski, W. (1997) Strand Specificity in the Interactions of *Escherichia coli* Primary Replicative Helicase DnaB Protein With Replication Fork, *Biochemistry 36*, 10320−10326.
17. Jezewska, M. J., Rajendran, S., and Bujalowski, W. (1998) Functional and Structural Heterogeneity of the DNA Binding of the *E. coli* Primary Replicative Helicase DnaB protein, *J. Biol. Chem. 273*, 9058−9069.
18. Jezewska, M. J., Rajendran, S., Bujalowska, D., and Bujalowski, W. (1998) Does ssDNA Pass Through the Inner channel of the Protein Hexamer in the Complex with the *E. coli* DnaB Helicase? Fluorescence Energy Transfer Studies, *J. Biol. Chem. 273*, 10515−10529.
19. Jezewska, M. J., Rajendran, S., and Bujalowski, W. (1998) Complex of *Escherichia coli* Primary Replicative Helicase DnaB Protein with a Replication Fork. Recognition and Structure, *Biochemistry 37*, 3116−3136.
20. Yu, X., Hingorani, M. M., Patel, S. S., and Egelman, E. H. (1996) DNA Is Bound Within the Central Hole to One Or Two of the Six Subunits of the DNA Helicase, *Nat. Struct. Biol. 3*, 740−743.
21. Dong, F., Gogol, E. P., and von Hippel, P. H. (1995) The Phage T4-coded DNA Replication Helicase (gp41) Forms a Hexamer upon Activation by Nucleoside Triphosphate, *J. Biol. Chem. 270*, 7462−7473.
22. Gogol, E. P., Seifried, S. E., and von Hippel, P. H. (1991) Structure and Assembly of the *Escherichia coli* Transcription Termination Factor Rho and its Interactions with RNA. I. Cryoelectron Microscopy Studies, *J. Mol. Biol. 221*, 1127−1138.
23. Jezewska, M. J., Galletto, R., and Bujalowski, W. (2004) Interactions of the RepA helicase hexamer of plasmid RSF1010 with the ssDNA. Quantitative Analysis of Stoichiometries, Intrinsic Affinities, Cooperativities, and Heterogeneity of the Total ssDNA-binding Site, *J. Mol. Biol. 343*, 115−136.
24. West, S. C. (1996) DNA Helicases: New Breeds of Translocating Motors and Molecular Pumps, *Cell 86*, 177−180.
25. Egelman, E. H., Yu, X., Wild, R., Hingorani, M. M., and Patel, S. S. (1995) Bacteriophage T7 Helicase/Primase Proteins Form Rings Around Single-Stranded DNA that Suggests a General Structure for Hexameric Helicases, *Proc. Natl. Acad. Sci. U.S.A. 92*, 3869−3873.
26. Trakselis, M. A., McGeoch, A. T., Laskey, R. A., and Bell, S. D. (2005) Organization of an Archaeal MCM Complex on DNA and Implications for a Helicase Mechanisms, *Nat. Struct. Mol. Biol. 12*, 756−762.
27. Richardson, J. P. (2003) Loading Rho to Terminate Transcription, *Cell 114*, 157−159.
28. Valle, M., Chen, X. S., Donate, L. E., Fanning, E., and Carazo, J. M. (2006) Structural Basis for the Cooperative Assembly of Large T Antigen on the Origin of Replication, *J. Mol. Biol. 357*, 1295−1305.
29. Wang, Y., and von Hippel, P. H. (1993) *Escherichia coli* Transcription Termination Factor Rho. 1. ATPase Activation by Oligonucleotide Cofactors, *J. Biol. Chem. 268*, 13940−13946.
30. SenGupta, D. J., and Borowiec, J. A. (1992) Strand-specific Recognition of a Synthetic DNA Replication Fork by the SV40 Large Tumor Antigen, *Science 256*, 1656−1661.
31. McSwiggen, J. A., Bear, D. G., and von Hippel, P. H. (1988) Interactions of *Escherichia coli* transcription termination factor Rho with RNA. I. Binding Stoichiometries and Free Energies, *J. Mol. Biol. 199*, 609−622.
32. Geiselmann, J., Wang, Y., Seifried, S. E., and Von Hippel, P. H. (1993) A Physical Model For the Translocation and Helicase Activities of *Escherichia coli* Transcription Termination Protein Rho, *Proc. Natl. Acad. Sci. U.S.A. 90*, 7754−7758.
33. San Martin, M. C., Stamford, N. P. J., Dammerova, N., Dixon, N. E., and Carazo, J. M. (1995) A Structural Model for the *Escherichia coli* DnaB Helicase Based on Electron Microscopy Data, *J. Struct. Biol. 114*, 167−176.
34. Yu, X., Jezewska, M. J., Bujalowski, W., and Egelman, E. H. (1996) The Hexameric *E. coli* DnaB Helicase can Exist in Different Quaternary States, *J. Mol. Biol. 259*, 7−14.
35. Yang, S., Yu., X., VanLoock, M. S., Jezewska, M. J., Bujalowski, W., and Egelman, E. H. (2002) Flexibility of the Rings: Structural Asymmetry in the DnaB Hexameric Helicase, *J. Mol. Biol. 321*, 839−849.
36. Bujalowski, W., and Jezewska, M. J. (2000) Kinetic Mechanism of the Single-Stranded DNA Recognition by *Escherichia coli* Replicative Helicase DnaB Protein. Application of the Matrix Projection Operator Technique to Analyze Stopped-Flow Kinetics, *J. Mol. Biol. 295*, 831−852.
37. Edelhoch, H. (1967) Spectroscopic Determination of Tryptophan and Tyrosine in Proteins, *Biochemistry 6*, 1948−1954.
38. Gill, S. C., and von Hippel, P. H. (1989) Calculation of Protein Extinction Coefficients from Amino Acid Sequence Data, *Anal. Biochem. 182*, 319−326.
39. Lucius, A. L., Jezewska, M. J., and Bujalowski, W. (2006) The *Escherichia coli* PriA Helicase Has Two Nucleotide-Binding Sites Differing in Their Affinities for Nucleotide Cofactors. 1. Intrinsic Affinities, Cooperativities, and Base Specificity of Nucleotide Cofactor Binding, *Biochemistry 45*, 7202−7216.
40. Jezewska, M. J., Rajendran, S., and Bujalowski, W. (1998) Transition between Different Binding Modes in Rat DNA Polymerase β-ssDNA Complexes, *J. Mol. Biol. 284*, 1113−1131.
41. Galletto, R., Maillard, R., Jezewska, M. J., and Bujalowski, W. (2004) Global Conformation of the *Escherichia coli* Replication Factor DnaC Protein in Absence and Presence of Nucleotide Cofactors, *Biochemistry 43*, 10988−11001.
42. Galletto, R., Jezewska, M. J., and Bujalowski, W. (2003) Interactions of the *Escherichia coli* DnaB Helicase Hexamer with the Replication Factor of the DnaC Protein. Effect of Nucleotide Cofactors and the ssDNA on Protein-Protein Interactions and the Topology of the Complex, *J. Mol. Biol. 329*, 441−465.
43. Stafford, W., III (1992) Boundary Analysis in Sedimentation Transport Experiments: A Procedure for Obtaining Sedimentation Coefficient Distributions Using the Time Derivative of the Concentration Profile, *Anal. Biochem. 203*, 295−301.
44. Correia, J. J., Chacko, B. M., Lam, S. S., and Lin, K. (2001) Sedimentation Studies Reveal a Direct Role of Phosphorylation in Smad3:Smad4 Homo- and Hetero-Dimerization, *Biochemistry 40*, 1473−1482.
45. Tanford, C. (1961) in *Physical Chemistry of Macromolecules*, pp 364−390, John Wiley & Sons, Inc., New York.
46. Cantor, R. C., and Schimmel, P. R. (1980) in *Biophysical Chemistry*, Vol. II, pp 591−641, W. H. Freeman, New York.
47. Jezewska, M. J., and Bujalowski, W. (1996) A General Method of Analysis of Ligand Binding to Competing Macromolecules Using the Spectroscopic Signal Originating from a Reference Macromolecule. Application to *Escherichia coli* Replicative Helicase DnaB Protein-Nucleic Acid Interactions, *Biochemistry 35*, 2117−2128.

48. Bujalowski, W., and Jezewska, M. J. (2000) *Spectrophotometry & Spectrofluorimetry. A Practical Approach* (Gore, M. G., Ed.) pp 141−165, Oxford University Press, New York.
49. Bujalowski, W., and Klonowska, M. M. (1994) Structural Characteristics of the Nucleotide Binding Site of the *E. coli* primary replicative Helicase DnaB Protein. Studies with Ribose and Base-Modified Fluorescent Nucleotide Analogs, *Biochemistry 33*, 4682−4694.
50. Jezewska, M. J., and Bujalowski, W. (1997) Quantitative Analysis of Ligand-Macromolecule Interactions Using Differential Quenching of the Ligand Fluorescence to Monitor the Binding, *Biophys. Chem. 64*, 253−269.
51. Bujalowski, W. (2006) Thermodynamic and Kinetic Methods of Analyses of Protein−Nucleic Acid Interactions. From Simpler to More Complex Systems, *Chem. Rev. 106*, 556−606.
52. Lakowicz, J. R. (1999) in *Principles of Fluorescence Spectroscopy*, pp 25−61, Plenum Press, New York.
53. Azumi, T., and McGlynn, S. P. (1962) Polarisation of the Luminescence of Phenantrene, *J. Chem. Phys. 37*, 2413−2420.
54. Jezewska, M. J., Galletto, R., and Bujalowski, W. (2003) Tertiary Conformation of the Template-Primer and Gapped DNA Substrates in Complexes with Rat Polymerase β. Fluorescence Energy Transfer Studies Using the Multiple Donor-Acceptor Approach, *Biochemistry 42*, 11864−11878.
55. Berman, H. A., Yguerabide, J., and Taylor, P. (1980) Fluorescence Energy Transfer on Acethylcholinesterase: Special Relationship between Peripheral Site and Active Center, *Biochemistry 19*, 2226−2235.
56. Dale, R. E., Eisinger, J., and Blumberg, W. E. (1979) The Orientation Freedom of Molecular Probes. The Orientation Factor in Intramolecular Energy Transfer, *Biophys. J. 26*, 161−194.
57. Seifried, S. E., Wang, Y., and von Hippel, P. H. (1988) Fluorescence Modification of the Cysteine 2002 Residues of *Escherichia coli* Transcription Termination Factor Rho, *J. Biol. Chem. 263*, 13511−13514.
58. Saenger, W. (1984) in *Principles of Nucleic Acid Structure*, pp 255−305, Springer-Verlag, New York.
59. Bloomfield, V. A., Crothers, D. M., and Tinoco, I. (1999) in *Nucleic Acid. Structures, Properties, and Functions*, pp 79−110, University Science Books, Sausalito, CA.
60. Bujalowski, W., and Klonowska, M. M. (1994) Close Proximity of Tryptophan Residues and ATP Binding Site in *Escherichia coli* Primary Replicative Helicase DnaB Protein. Molecular Topography of the Enzyme, *J. Biol. Chem. 269*, 31359−31371.
61. Lee, J. C., and Timasheff, S. N. (1979) The Calculation of Partial Specific Volumes of Proteins in 6 M Guanidine Hydrochloride, *Methods Enzymol. 61*, 49−57.
62. Kuntz, I. D. (1971) Hydration of Macromolecules III. Hydration of Polypeptides, *J. Am. Chem. Soc. 93*, 514−516.
63. Galletto, R., Jezewska, M. J., and Bujalowski, W. (2004) Unzipping Mechanism of the Double-Stranded DNA Unwinding by a Hexameric Helicase. I. Quantitative Analysis of the Rate of the dsDNA Unwinding, Processivity and Kinetic Step-Size of the *Escherichia coli* DnaB Helicase Using Rapid Quench-Flow Method, *J. Mol. Biol. 343*, 83−99.
64. Galletto, R., Jezewska, M. J., and Bujalowski, W. (2004) Unzipping Mechanism of the Double-Stranded DNA Unwinding by a Hexameric Helicase. II. The Effect of the 3′ Arm and the Stability of the dsDNA on the Unwinding Activity of the *Escherichia coli* DnaB Helicase, *J. Mol. Biol. 343*, 101−114.
65. Yang, M., and Millar, D. P. (1997) Fluorescence Resonance Energy Transfer as a Probe of DNA Structure and Function, *Methods Enzymol. 278*, 417−444.
66. Bailey, M. F., Thompson, E. H., and Millar, D. P. (2001) Probing DNA Polymerase Fidelity Mechanisms Using Time-Resolved Fluorescence Anisotropy, *Methods 25*, 62−77.
67. Vamosi, G., and Clegg, R. M. (1998) The Helix-Coil Transition of DNA Duplexes and Hairpins Observed by Multiple Fluorescence Parameters, *Biochemistry 37*, 14300−14316.
68. Trakselis, M. A., Alley, S. C., Able-Santos, E., and Benkovic, S. J. (2001) Creating a Dynamic Picture of the Sliding Clamp During T4 DNA Polymerase Holoenzyme Assembly by Using Fluorescence Resonance Energy Transfer, *Proc. Natl. Acad. Sci. U.S.A. 98*, 8368−8375.
69. Parkhurst, L. J. (2004) Distance Parameters Derived from Time-Resolved Forster Resonance Energy Transfer Measurements and Their Use in Structural Interpretations of Thermodynamic Quantities Associated with Protein-DNA Interactions, *Methods Enzymol. 379*, 235−262.
70. Jezewska, M. J., Rajendran, S., and Bujalowski, W. (2000) *Escherichia coli* Helicase PriA Protein-Single Stranded DNA Complex, *J. Biol. Chem. 275*, 27865−27873.
71. Jezewska, M. J., Rajendran, S., and Bujalowski, W. (2000) Interactions of *Escherichia coli* Replicative Helicase PriA Protein with Single-Stranded DNA, *Biochemistry 39*, 10454−10467.

BI700729K